Lake Surface Temperature Dataset in the North Slave Region Retrieved from Landsat Satellite Series - 1984 to 2021

Gifty Attiah [1,2], Homa Kheyrollah Pour [1,2], K. Andrea Scott [3]

[1]Remote Sensing of Environmental Change (ReSEC) Research group, Department of Geography and Environmental Studies, Wilfrid Laurier University, 75 University Ave, West N2L 3C5, Canada
[2]Cold Regions Research Centre, Wilfrid Laurier University, Waterloo, ON, Canada
[3] Department of Systems Design Engineering, University of Waterloo, 200 University Ave, West N2L 3G1, Canada

Correspondence to: Gifty Attiah (gattiah@wlu.ca)

Abstract. Lake surface temperature (LST) is an important attribute that highlights regional weather and climate variability and trends. The spatial resolution and thermal sensors on Landsat platforms provide the capability of monitoring the temporal and spatial distribution of lake surface temperature on small to medium size lakes. In this study, a retrieval algorithm was applied to the thermal bands of Landsat archives to generate an LST dataset (North Slave LST dataset) for 535 lakes in the North Slave Region (NSR) of the Northwest Territories (NWT), Canada, for the period of 1984 to 2021. North Slave LST was retrieved from Landsat-5 TM, Landsat-7 ETM+ and Landsat-8 OLI/TIRS; however, most of the dataset was created from the thermal bands of Landsat-5 (43%) due to its longevity (1984-2013). Cloud masks were applied to Landsat images to eliminate cloud cover. In addition, a 100-meter inward buffer was applied to lakes to prevent pixel mixing with shorelines. To evaluate the algorithm applied, retrieved LST was compared with in-situ data and Moderate Resolution Imaging Spectroradiometer (MODIS) LST observations. A good agreement was observed between in-situ observations and North Slave LST derived in this study with a mean bias of 0.12 °C and an RMSD of 1.7 °C. The North Slave LST dataset contains more available data for warmer months (May to September), covering 57.3 % compared to colder months (October to April). The average number of images per year for each lake across the NSR ranged from 20 to 45. The North Slave LST dataset will provide communities, scientists and stakeholders with spatial and temporal changing temperature trends on lakes for the past 38 years.
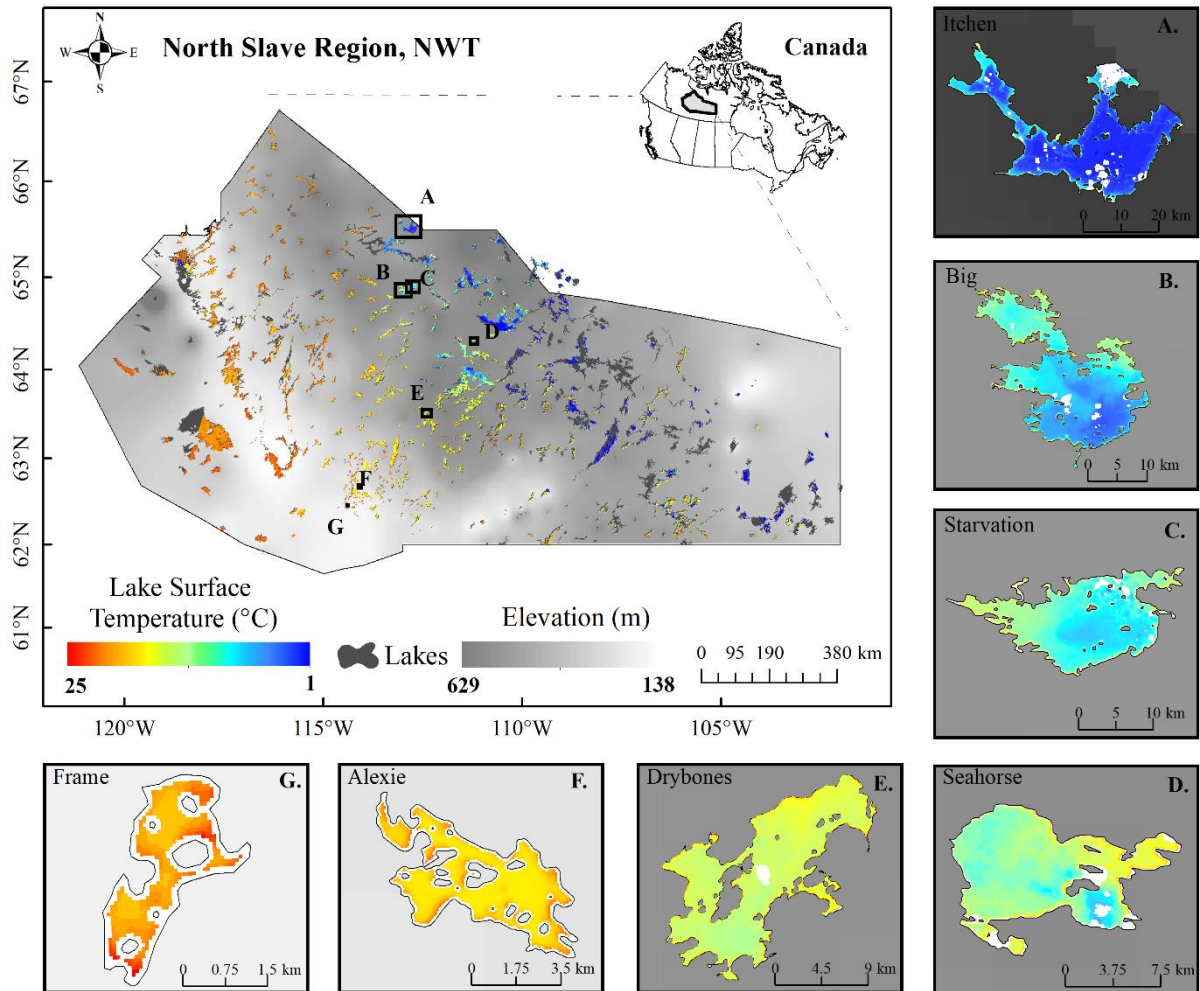
1 Introduction

25 Lake surface temperature (LST) is a significant indicator of climate change and is crucial to lake ecosystems (Livingstone et al., 2005; G. Zhang et al., 2019). Several ecological, biological, and hydrogeochemical processes are influenced by temperature in lakes (Schneider & Hook, 2010). Lake warming can result in a decrease in ice cover, changes in over-lake wind speeds, and changes in water column stratification (Austin & Colman, 2007; Desai et al., 2009; Kraemer et al., 2015; Magnuson et al., 2000). Land-water-atmosphere system's energy and material exchange processes can also be reflected in lake surface
30 temperature (Huang et al., 2017; Yang et al., 2020) and hence recognised as an essential climate variable. As a significant

variable in regional studies, the impact and relationship of LST to weather, climate and lake processes have been explored by other studies, including influences on the weather (Kheyrollah Pour et al., 2014a,b; Eerola et al., 2014; Kheyrollah Pour et al., 2017), climate (Moigne et al., 2016; Wang et al., 2021), precipitation (Zhang et al., 2016), lake effect snow (Shi & Xie, 2019) and lake overturning (Fichot et al., 2019). Observations of lakes around the world have reported increases in lake temperature
35   associated with global warming resulting in changes to the underlying lake system (O'Reilly et al., 2015; Woolway et al., 2019). Long-term records of lake surface temperature are therefore necessary to understand the thermal mechanism underlying lake processes, including lake ice formation and decay, lake productivity, aquatic ecosystems and other limnological processes (Chen et al., 2019; Collingsworth et al., 2017; Woolway et al., 2020).

Even though in-situ records on lake surface temperatures are a good source of temperature data for lake studies, their sparse
40   distribution, especially in the north, presents a challenge, making satellite-derived data an essential resource in regional and global studies. Satellite sensors like MODIS (Moderate Resolution Imaging Spectroradiometer) and AVHRR (Advanced Very High-Resolution Radiometer) have been heavily relied upon to estimate and analyse LST in several studies (*e.g.,* Kheyrollah Pour et al., 2012, 2014a, b, 2017; Reinart & Reinhold, 2008; Sima et al., 2013; Wan et al., 2002; Wloczyk et al., 2006; Zhao et al., 2020); however, their application to small and medium lakes is limited due to relatively moderate spatial resolution
45   (~250 m - 1 km). In addition, satellite-retrieved LST datasets for global studies like the Global Lake Temperature Collaboration (GLTC) have a low sampling of high-latitude lakes, restricting their use for climate studies in these northern regions. Satellites like Landsat, however, provide an opportunity for regional studies of lake processes and spatial extraction of LST, including Arctic and subarctic lakes. The strength of Landsat includes its high spatial resolution (30 m -120 m), high radiometric resolution (8-12 bits) and the presence of thermal infrared bands for the retrieval of LST. In addition, the longevity of data
50   archives makes it one of the most extensive and extended observations of earth's surface water from space (Pekel et al., 2016). Currently, a regional spatial lake surface temperature dataset for small and medium size lakes on a large scale does not exist in NWT, specifically for North Slave Region (NSR) lakes. This study seeks to bridge this gap by using the capabilities of Landsat to achieve this.

In this study, we generated LST data (North Slave LST) for over 535 predominantly small to medium lakes using data obtained
55   from Landsat archives (Landsat-5 TM, Landsat-7 ETM+ and Landsat-8 OLI/TIRS). An adapted temperature retrieval algorithm (Jimenez-Munoz et al., 2009, 2014) is applied to the thermal bands of Landsat to estimate LST. The dataset produced has a spatial resolution of 30 m and varying temporal resolution due to differences in satellite overpass and cloud interference. The generated North Slave LST dataset was evaluated with in-situ datasets and compared with the widely used LST satellite dataset (MODIS). The temporal and spatial distribution of the dataset is presented to report on data availability patterns.
60   Additionally, the North Slave LST dataset is used to briefly highlight the spatial inter-lake and intra-lake distribution of LST in the NSR lakes.

This study aims to (i) capitalise on the thermal bands of Landsat to create an up-to-date lake surface temperature dataset in the NSR to record distribution from 1984 to 2021; (ii) highlight the temporal and spatial heterogeneity of LST between and within

lakes on a 30 m grid; (iii) Distribute and publish LST data for stakeholders, research communities to facilitate further research
65 and studies, the public and the Government of the Northwest Territories to facilitate decision-making processes.

2 Study Lakes and Data Sources

2.1 Selected Lakes in North Slave Region, NWT

The North Slave LST data is generated for 535 lakes, between latitude 61°N and 67°N and longitude -120°W and -102W of the Northwest Territories (NWT) located in the northern part of Canada covering an area of about 316,000 km^2 (Figure 1 a).
70 The region lies in the Slave province of the Canadian shield and is interspersed with numerous lakes (>10,000) of various sizes. Elevation in the NSR has an average altitude of 301 m, with lake elevation ranging from 138 m to 624 m (Messager et al., 2016). This dataset contains 535 lakes with surface areas ranging from 0.05 km^2 to 1680 km^2 and mean depths ranging from 1 m – 63 m with volumes ranging from 0.24 km^3 to 27321 km^3. Appendix A contains a list of lakes with geophysical properties. Air temperature in the NSR ranges from ~-45°C to +30°C. The majority of the study lakes are between 1 and 5 km^2
75 (Figure 1b), and the dominant mean depth range was 5 – 10 m (Figure 1c).
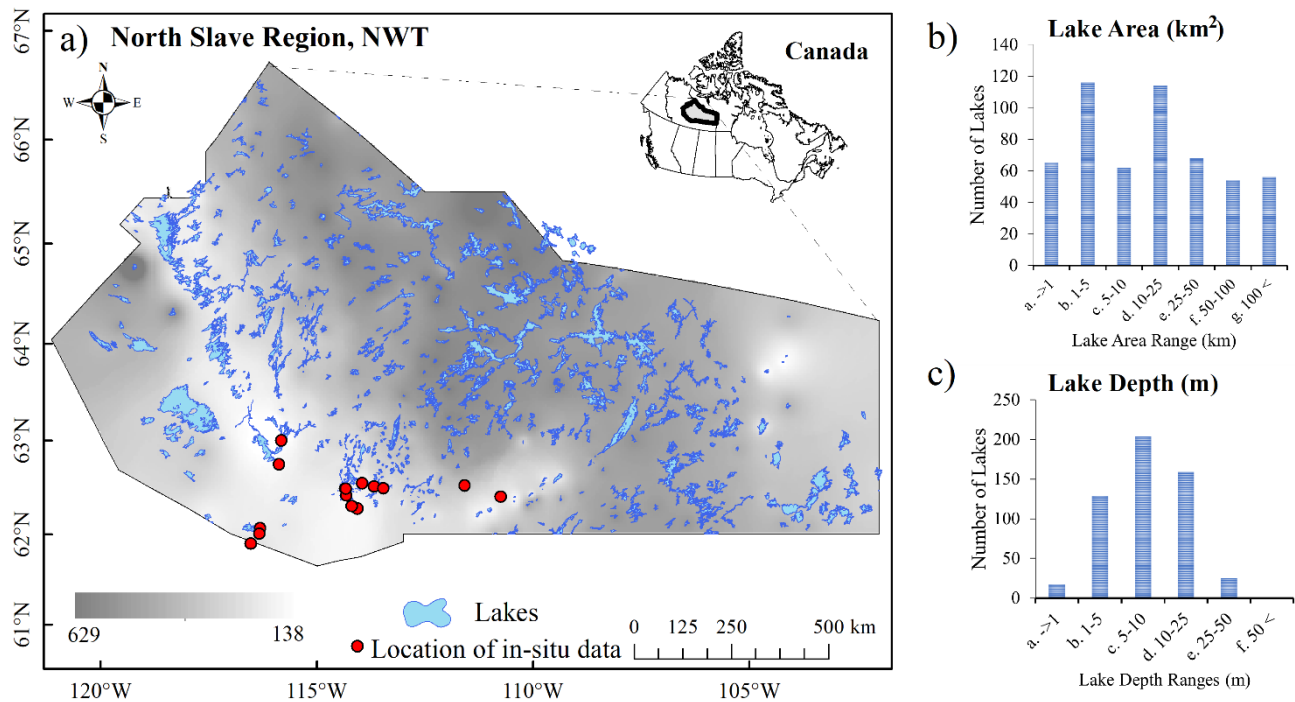

Figure 1: Geographic distribution of study lakes in the North Slave Region, Northwest Territories, Canada. The lakes area and depth distribution are shown in b) and c), respectively.

2.2 Spatial Data for LST Retrieval

2.2.1 Landsat Archives

Landsat archives consist of optical data from a series of earth-observing satellite missions. For this study, Landsat data was obtained from the United States Geological Survey (USGS) across the NSR. Landsat thermal bands were used to estimate surface temperature on lakes from the thermal infrared (TIR) bands of Landsat-5 TM (Thematic Mapper) (1984-2013), Landsat-7 ETM+ (Enhanced Thematic Mapper Plus) (1999-present) and Landsat-8 OLI/TIRS (Operational Land Imager and the Thermal Infrared Sensor) (2013-present) instruments. Landsat instruments orbit at an altitude of 705 km, are sun-synchronous and have a 16-day repeat cycle. The thermal band (band 6) of Landsat-5 and Landsat-7 record emitted radiation between the wavelengths of 10.40 µm to12.50 µm while that of Landsat-8 (band 10) records in band 10 between 10.6 µm to 11.19 µm. The spatial resolution of thermal bands Landsat-5 TM (120 m), Landsat-7 ETM+ (60 m) and Landsat-8 OLI/TIRS (100 m) are resampled with the cubic convolution method and distributed at a spatial resolution of 30 m to match optical bands (USGS, 2022). In addition, other bands, including the quality band (BQA), near-infrared band and the red bands, in addition to metadata, are also used in the retrieval of LST. About 34 Landsat tiles scenes cover the NSR, with each tile containing 5000 × 5000 30 m pixels and overpass times ranging between 18:00 to 20:00 UTC.

2.2.2 ERA5 Reanalysis Data

Total column water vapour from ERA5 reanalysis data (Copernicus Climate Change Service (C3S), 2017) from 1984 to 2021 was used as input in the algorithm to correct for atmospheric effects on Landsat images. Data were derived from the hourly data with a ~30 km spatial resolution from the European Centre for Medium-Range Weather Forecasts (ECMWF) (Hersbach et al., 2020). ERA5 reanalysis data is a dataset generated from a combination of in-situ observations and modelling to provide estimates of land, atmospheric and ocean changes on a global scale. Average ERA5 hourly total column water vapour on single levels was used in the LST retrieval algorithm

2.2.3 Lake Outline and Properties Data

The name, location, depth, size, elevation, and outline of each lake were retrieved from a combination of the HydroLAKES database, CanVec series and the Water file-Lakes and Rivers database. HydroLAKES database is a digital map repository developed in the Global HydroLAB (http://wp.geog.mcgill.ca/hydrolab/) from a collection of several databases (*e.g.,* Global and regional databases like CanVec series and SRTM Water Body Data (Slater et al., 2006)). This database provides information on world lakes and their significant properties through high-resolution maps. Over 1,427,688 individual lake vector polygons greater than 10 ha are included in the repository (Messager et al., 2016). The mode of pixel-level lake elevation data was obtained from the Earth-Env-DEM90 digital elevation model and the USGS-provided GTOPO30 DEM is used to calculate HydroLAKES elevation data. A geostatistical model developed from surrounding land surface topography was derived to generate average lake depths and volumes (Messager et al., 2016). As part of the Government of Canada initiative

(https://open.canada.ca), the CanVec series provides a geometric description and fundamental characteristics of hydrographic phenomena in the form of geospatial vector data. The Water file-Lakes and Rivers polygons data (https://www12.statcan.gc.ca) maps lakes and rivers under the 2006 census, created by statistics Canada under the Government of Canada on August 29, 2013. This data was the primary source of lake names attributed to lake outlines in our dataset.

2.2.4 Evaluation Dataset

Landsat-derived LST was generated during both open-water and ice-covered seasons. Retrieved data were evaluated against in-situ measurements collected over selected locations within the study area (Figure 1). In-situ measurements from Mackenzie DataStream were used for evaluating LST derived from Landsat. DataStream is an open-access freshwater data platform that provides water monitoring data collected by governments and communities across Canada (Environment and Climate Change Canada, 2020). The database for the NWT region was the product of the NWT-wide community-based water quality monitoring (CBM) program, which is collected during open water seasons. The CBM program was implemented in 2012 as a partnership between the Department of Environment and Natural Resources (ENR), the Government of the Northwest Territories (GNWT), communities and regional organisations in NWT to monitor water quality and changes. The surface temperature of lakes was measured with YSI Sondes and EXO 2 Sondes and interpreted by ENR. Collated surface temperature data used for evaluation from this source was from the years 2014 to 2019. Another primary source was lake temperature data collected by Environment and Climate Change Canada (ECCC) from 1999 to 2003. Temperature loggers were used to measure hourly temperature on lakes for given periods during open water periods; however, only temperature collected at the skin surface (depth= 0 m) was used for LST evaluation in this study.

MODIS (MYD11_L2) surface temperature dataset from 2003 to 2021 was used to evaluate Landsat-derived LST data generated during both open water and ice-covered seasons. The dataset was obtained from NASA's Earth Observing System Data and Information System (EOSDIS), mounted on terra and aqua satellites, MODIS records within the spectral ranges of 0.405 - 14.385 μm across 36 bands. The aqua product contains nighttime, and daytime LST measurements on a spatial resolution of ~1 km derived from the thermal infrared bands. For this study, the daytime LST measurement covering lakes in the NSR was compared against the Landsat-derived LST.

3. Methods

3.1 Algorithm for Lake Surface Temperature

The thermal bands of Landsat were used in the retrieval algorithm to generate North Slave LST (band 6 for Landsat-5TM/Landsat-7ETM+ and band 10 for Landsat OLI/TIRS). Atmospheric and emissivity correction of thermal bands were conducted to account for the effect of absorption and emission on surface radiation. A single channel (SC) method was adapted and applied in this study to retrieve LST (Jimenez-Munoz et al., 2009, 2014; Jiménez-Muñoz & Sobrino, 2003). This method is based on approximating the radiative transfer equation without the dependence on in-situ radio-sounding data. A single band

is used in the SC method, making it feasible for single thermal band satellites like Landsat-5 TM, which was used in this study. SC method uses atmospheric water vapour (Sect. 2.2.2) as a variable in the correction for atmospheric effect.

LST retrieval using the SC method requires atmospheric water vapour, emissivity, brightness temperature and wavelength emitted radiance values, and thermal constants. LST estimation is based on the following Eq. (1) (Jiménez-Munoz & Sobrino, 2003):

$$LST = \gamma\left[\varepsilon^{-1}(\psi_1 L_{sensor,\lambda} + \psi_2) + \psi_3\right] + \delta , \tag{1}$$

where:

$$\gamma = \left\{\frac{c_2 L_{sensor,\lambda}}{T_{sensor}^2}\left[\frac{\lambda^4}{c_1}L_{sensor,\lambda} + \lambda^{-1}\right]\right\}^{-1} , \tag{2}$$

and:

$$\delta = -\gamma L_{sensor,\lambda} + T_{sensor} , \tag{3}$$

At-sensor radiance and brightness temperature are denoted by $L_{sensor,\lambda}$ (W m^{-2} sr^{-1} μm^{-1}) and T_{sensor} (K) respectively. c_1 (1.19104 10^8 W μm^4 m^{-2} sr^{-1}) and c_2 (14387.7 μm K) are Plank's constants. Emitted radiance wavelength (λ) is 11.457 μm in Landsat-5 TM, 11.269 μm in Landsat-7 ETM+ and 10.904 μm in Landsat-8 OLI TIRS. ψ_1, ψ_2 and ψ_3 are atmospheric functions obtained as a function of water vapour (w) and are specific to the three individual Landsat sensors.

At-sensor spectral radiance was calculated from raw digital numbers (DN) of thermal bands based on metadata information and constants. Equations used are specific to the type of sensor, as listed below.

At-sensor radiance values for Landsat-5 TM were derived using Eq. (4) (Chander & Markham, 2003):

$$L_{sensor,\lambda} = G_{rescale}. DN + B_{rescale} , \tag{4}$$

where 0.0551584 Wm^{2}sr^{1}μm^1/DN and 1.2378 Wm^{2}sr^{1}μm^1/DN are constants for $G_{rescale}$ and $B_{rescale,}$ respectively.

Landsat-7 ETM+ was derived using Eq. (5) (Ihlen & Zanter, 2019) :

$$L_{sensor,\lambda} = \left(\frac{L_{\lambda max} - L_{\lambda min}}{Q_{calmax} - Q_{calmin}}\right)(Q_{cal} - Q_{calmin}) + L_{\lambda min} , \tag{5}$$

where the maximum and minimum spectral radiance is represented by $L_{\lambda max}$ and $L_{\lambda min,}$ respectively, and the maximum and minimum quantised calibrate pixel is represented by Q_{calmax} and $Q_{calmin,}$ respectively, obtained from the metafile. Q_{cal} denotes DN values of pixels in band 6.

Landsat-8 OLI TIRS was derived using Eq. (6) (US Geological Survey, 2016):

$$L_{sensor,\lambda} = M_L Q_{cal} + A_L , \tag{6}$$

where DN values of pixels in band 10 are denoted by Q_{cal}. $M_L = 0.000342$, and $A_L = 0.1$ are fixed rescaling factors in the metadata provided by the USGS.

Brightness temperature T_{sensor} is estimated using calculated at-sensor radiance values and thermal constants derived from the metadata based on Eq. (7) below:

$$T_{sensor} = \frac{K_2}{ln\left(\frac{K_1}{L_{sensor,\lambda}}+1\right)},$$ (7)

where thermal constants K_1 (W m^{-2} sr^{-1} µm^{-1}) and K_2 (K) vary based on the type of Landsat sensor (Table 1).

Table 1: Thermal constants applied to Landsat thermal bands for brightness temperature estimation

Thermal Constant	Landsat-5 TM Band 6	Landsat-7 ETM+ Band 6	Landsat-8 OLI/TIRS Band 10
K_1	607.76	666.09	774.8853
K_2	1260.56	1282.71	1321.0789

Atmospheric Functions (AFs) used for atmospheric correction were based on coefficients acquired using Global Atmospheric Profiles from Reanalysis Information (GAPRI) and Thermodynamic Initial Guess Retrieval (TIGR) databases (Jimenez-Munoz et al., 2009, 2014).

Atmospheric Functions Equations ψ_1, ψ_2 and ψ_3 particularised for Landsat-8 OLI/TIRS 8 are:

$$\psi_1 = 0.04019w^2 + 0.02916w + 1.01523 ,$$ (8a)

$$\psi_2 = -0.38333w^2 - 0.50294w + 0.20324,$$ (8b)

$$\psi_1 = 0.00918w^2 + 1.36072w - 0.27514 ,$$ (8c)

Landsat-7 ETM+ AFs:

$$\psi_1 = 0.07593w^2 - 0.07132w + 1.08565 ,$$ (9a)

$$\psi_1 = -0.61438w^2 - 0.70916w - 0.19379 ,$$ (9b)

$$\psi_1 = -0.02892w^2 + 1.46051w - 0.43199 ,$$ (9c)

Landsat-5 TM AFs:

$$\psi_1 = 0.07518w^2 - 0.00492w + 1.03189 ,$$ (10a)

$$\psi_1 = -0.59600w^2 - 1.22554w + 0.08104 ,$$ (10b)

$$\psi_1 = -0.02767w^2 + 1.43740w - 0.25844 , \tag{10c}$$

Normalised Difference Vegetation Index (NDVI) (Eq.8) values calculated were used to assign surface lake surface emissivity. Infrared (NIR) and red bands of Landsat were used to calculate NDVI values with (Eq.11).

195 $$NDVI = \frac{NIR-Red}{NIR+Red} , \tag{11}$$

The lake surface was assigned an emissivity of 0.985 if NDVI values were lower than 0.05; otherwise, a value of 0.97 was assigned (Prats et al., 2018).

3.2 Retrieval of Lake Surface Temperature

3.2.1 Lake LST Retrieval

200 LST retrieval algorithms were applied to the thermal bands in conjunction with other processed output from Landsat data to generate the LST dataset. Quality Assurance (QA) band outlining surface, atmosphere, and sensor conditions included in the Landsat data were used to mask clouds and other obstructions. The QA band assesses cloud influence at different confidence levels [high (67-100 %), medium (34-66 %) and low (0-33 %)], making it possible for cloud removal. In this study, high and medium confidence values were categorised as cloud pixels, while low confidence was considered cloud-free. LST retrieval

205 algorithms and equations (Eq. 1 – Eq. 11) were applied to the thermal bands of all tiles from 1984 to 2021. Cloud masks were generated and applied to retrieved LST to eliminate cloud distorted pixels. LST pixels were extracted using vector files of lake outlines from the HydroLAKES datasets. A 100 m negative buffer was applied to remove the effect of lake pixel mixing with land surface pixels. Possible erroneous pixels were flagged using z-scores which calculate how far a value is from the mean and was used to access spatial differences and outliers in pixels. Pixels with z-score values of above 3.5 and below -3.5 of

210 lakes were flagged. In addition, LST output with equal pixels across the entire lake or group of pixels having the same value to four decimal places were flagged. Further visual quality checks and analysis were applied to flagged LST to clean generated data and remove erroneous cloud cover that could not be captured in masks. The overall framework for retrieval and generation of the LST dataset for selected lakes in the NSR is highlighted in Figure 2.
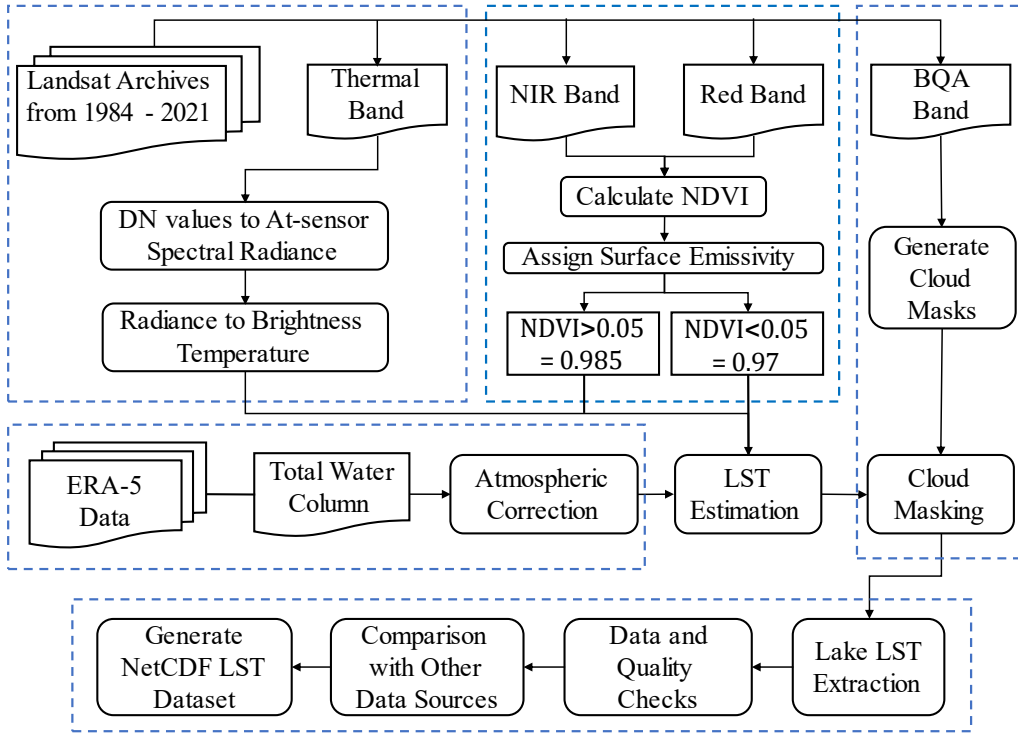
Figure 2: Workflow and methods for generating LST dataset from Landsat archives.

3.2.2 Data Quality Assessment Information

It is essential to highlight the limitations in data estimates from satellite-based records (Merchant et al., 2017). This provides awareness of the degree to which a sensor is stable and observations obtained from them. In addition, these reports are necessary to inform the confidence of data extracted and the structures of their errors through time and space. One significant distortion of Landsat archives is the failing of the scan line corrector of Landsat-7 ETM+ on May 31 2003. As a result, the measurement from scans could not be corrected, rendering all images sensed after that date losing about 22% of the data extracted. This limitation, named Landsat-7 ETM+ SLC-off issue, is more prominent on the edges of images than in the centre. Landsat-7 ETM+ data was still used in the study because the radiometric and geometric corrections are unaffected by this scan line issue.

3.2.3 Evaluation Methods

Indicators used to evaluate the performance of North Slave LST against in-situ and MODIS LST were the root mean squared deviation (RMSD), mean bias deviation (MBD) and R-squared. The MBD, which assesses systematic differences, evaluates the under-prediction and over-prediction between two datasets. An MBD value of 0 indicates an utterly random error.

10

$$MBD = \frac{\sum_{i=1}^{N}[P_i - O_i]}{N},$$ (12)

230 where Oi and Pi are the observed and predicted values, respectively, while N is the number of points used for evaluation. The index values ranged between 0 and 1, indicating the worst and best possible performance, respectively.

The root means squared deviation (RMSD) measures the total difference between two datasets without distinguishing between over or under-prediction of models/algorithms. No deviation in values results in an RMSD value of 0.

$$RMSD = \sqrt{\frac{\sum_{i=1}^{N}[P_i - O_i]^2}{N}},$$ (13)

235 **4 Results and Discussion**

4.1 Quality of Landsat-derived LST

The primary sources of limitation for North Slave LST products include (i) potential mixed pixels that might not be captured by the algorithm, (ii) the presence of *no data* pixels on lakes and (iii) inconsistency in the temporal resolution of dataset per lake. Lake boundaries extraction of LST was based on outlines from external boundary files (Sect. 2.2.4). As such, errors that
240 may exist, including overestimating lake area and incapability to accurately demarcate lake islands, would affect LST values retrieved. A 100-meter inward buffer was applied to address this; however, valuable lake shore LST information is lost, especially in small lakes. The number of pixels and the percentage of the lake it represents are reported in Appendix A. Depending on the lake shape, area and existence of islands, pixels represented 16.7% to 97.34% of the lake area. The spatial variation in LST is reduced for lakes with a smaller number of pixels.
245 In addition to the overall representativeness of pixels on lakes, LST pixels retrieved for a given day may vary due to cloud cover and Landsat-7 ETM+ SLC-off issue (Sect. 3.2.2). This results in missing LST pixels for a given lake. These pixels are represented with *no data* pixels (which do not contain LST values) in the dataset. Figure (3) highlights the fraction of LST pixels to *no data* pixels distributed over years and months. The percentage of *no data* pixels ranged from 30.6% (1996) to 45.4% (1993) across the years, with relatively lower *no data* pixels percentages recorded from 2014 to 2021 (less than 37.2%)
250 (Figure 3a). Generally, earlier years recorded higher *no data* pixels percentages compared to later years. For example, monthly distribution (Figure 3b) showed the least percentage of *no data* pixels for February (26.8%) and the highest for October (51.2%).
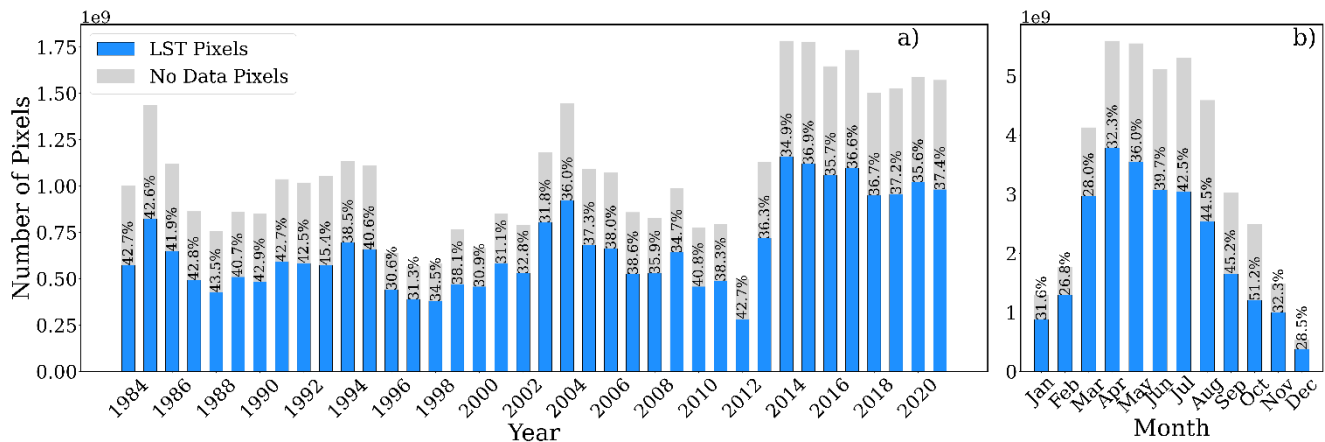
Figure 3: a) Year and b) monthly distribution of LST pixels vs *no data* pixels, highlighting the percentage of *no data* pixels for a given period.

Due to the presence of *no data* pixels, it is necessary to inform on the percentage coverage of LST pixels. LST pixel coverage for each image is calculated as - LST pixels retrieved divided by the number of total pixels for a given lake multiplied by 100 per cent. LST pixel coverage is reported for each lake on a given day as part of the naming and metadata of our dataset. Figure (4) shows the yearly distribution of LST pixel coverage for the entire dataset. Lakes with less than 10% of LST pixels on a given day were eliminated from the dataset. The percentage of lakes with LST pixel coverage greater than 90% was 47.2% (Figure 4a). A greater percentage (77.4%) of lakes in the dataset had more than 50% LST pixels coverage. The percentage of lakes with LST pixels coverage greater than 90% is plotted in Figure 4b annually. Results show a general reduction in percentage with time, where earlier years had higher percentages of LST pixels coverage > 90% than in recent years. This downward trend can be attributed to the Landsat-7 ETM+ SLC-off issue, which increases the presence of *no data* pixels.

Even though the typical overpass for Landsat is 16 days, the temporal resolution of the North Slave LST dataset varied due to the overlap of satellite sensors for specific years and the inability to retrieve LST due to the cloud cover. The distribution and frequency of the data were based on the operational times of the three Landsat satellites used in this study. Most of the LST dataset was derived from Landsat-5 (43%). Landsat-7 and Landsat-8 contributed 34% and 22% of the dataset, respectively. LST images from 1999 were derived from two sets of Landsat (Landsat-5 and Landsat-7 from 1999 to 2011) and (Landsat-7 and Landsat-8 from 2013 to 2021). Years with overlapping sensors may have shorter temporal resolution than years with only one sensor retrieval. As a result, there is an inconsistency with the temporal resolution of the LST product.

12
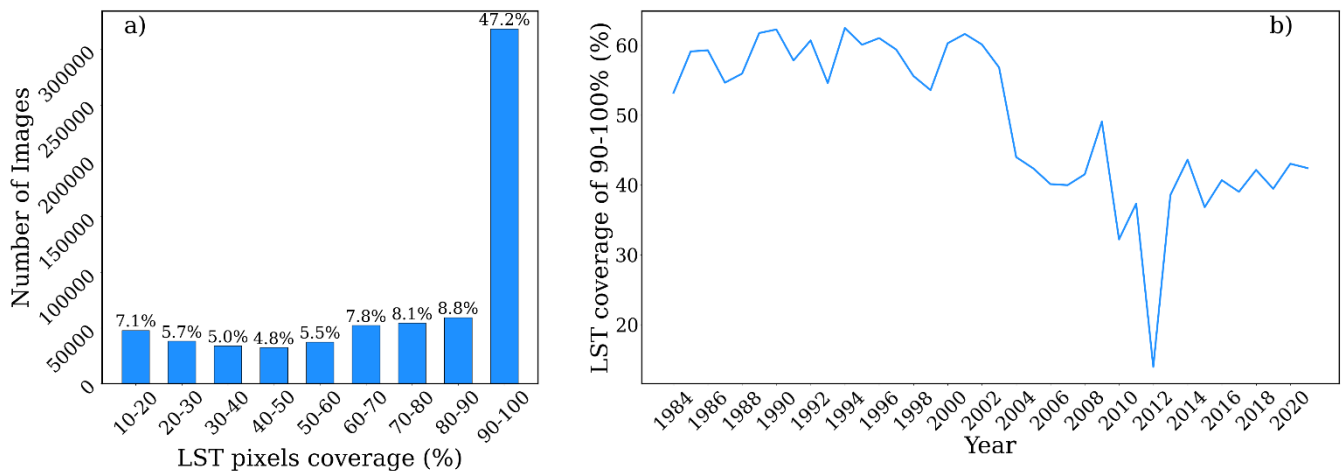
Figure 4: a) Distribution of LST pixels coverage (%) and b) yearly percentage of the dataset with LST coverage ranging from 90-100%.

4.2 North Slave LST dataset Evaluation

4.2.1 Evaluation of LST Data

The accuracy of generated North Slave LST was examined by evaluating Landsat-derived LST to corresponding in-situ data (Fig 5). Dates from both measured in-situ surface water temperature data (DataStream and ECCC) and derived North Slave LST data were matched up. In addition, a comparison with the generated dataset was conducted using the widely used daily MODIS LST. Ground-based observations were compared against equivalent pixels within which measurements were taken, and North Slave LST data were plotted against corresponding in-situ surface temperature measurements (Figure 5). A good correlation was observed between North Slave LST data and in-situ surface water temperature, with an R^2 value of 0.89 for the regression line. North Slave LST was slightly higher than in-situ records with an MBD of 0.12 and RMSD of 1.71 °C.

Deviations between North Slave LST and measured surface water temperature could be due to differences between image acquisition times and the time of the in-situ measurements. Landsat capture times of the NSR ranged between 18:00 and 20:00 UTC, corresponding to 12:00 - 14:00 local time. However, the time of in-situ observations was variable and did not necessarily correspond to the time of satellite image acquisition. Further variations in North Slave LST can also be attributed to the differences in sample collection and spatial resolution. North Slave LST is essentially the mean of ~60 to 120 m^2 area instead of a single in-situ location. Possible errors reported by other studies for the differences in measured and Landsat values include georeferencing, radiometric and memory effects (Chander & Markham, 2003; Markham et al., 2014; Sentlinger et al., 2008; USGS,2022, Young et al., 2017).

13
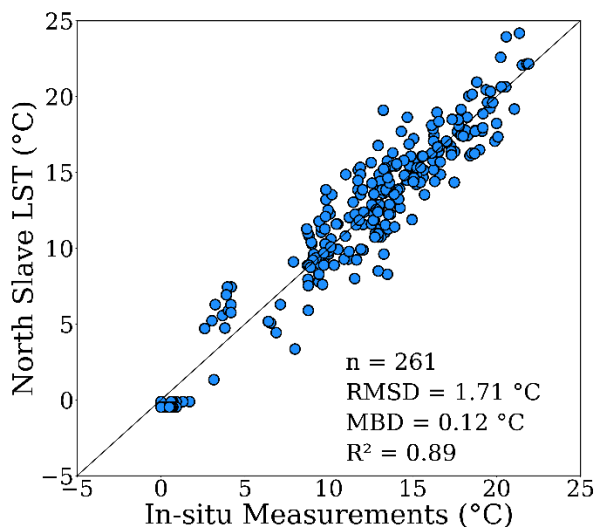
Figure 5: Comparison of North Slave LST with DataStream and ECCC in-situ measurements of water surface temperature during open water seasons.

Statistical parameters, including average yearly LST for open water season, total average LST and variance, were calculated for available ECCC and DataStream in-situ data and compared against North Slave LST, which is highlighted in Table 2. Absolute differences calculated for the statistical parameters ranged from 0.1°C to 1°C. The highest absolute difference for the average LST for open water between the two datasets was 1°C calculated for the year 2000 of the ECCC data. The variance was 0.6°C and 0.3°C for the ECCC and Datastream, respectively. Differences between the total LST average were the lowest, with 0.3°C and 0.1°C from 1999 to 2003 and 2014 to 2019, respectively.

Table 2: Comparison of yearly average LST, average LST and variance between North Slave LST and In-Situ LST.

Statistical Parameters	Data	Period	In-Situ LST (°C)	North Slave LST (°C)	Absolute Difference (°C)
Average LST for open water season (June – September)	ECCC	1999	11.9	12.2	0.3
		2000	10.8	11.8	1
		2001	13.7	14.2	0.5
		2002	11.1	11.2	0.1
		2003	12.2	12.5	0.3
	DataStream	2014	13.7	14.2	0.5
		2015	15.1	14.5	0.6
		2016	16.1	16.4	0.3
		2017	15	15.5	0.5
		2019	14.2	13.3	0.9
Total LST Average for open water season	ECCC	1999-2003	12.3	12.6	0.3
	DataStrean	2014-2019	14.9	14.8	0.1
Variance	ECCC	1999-2003	15.5	14.9	0.6
	DataStream	2014-2019	3.8	4.1	0.3

14

4.2.2 Yearly and Monthly Comparison of LST data to MODIS Data

MODIS LST was first compared against available water surface temperature measurements from DataStream (Figure 6a) and Landsat-derived LST for days when records were available from all three data sources. The aim was to compare the deviation of Landsat-derived LST and water surface temperature to that of MODIS and water surface temperature. A relatively low
310   coefficient of determination was observed for MODIS LST ($R^2 = 0.5$) compared to Landsat-derived LST ($R^2 = 0.94$) when evaluated against water surface temperature. RMSD values were also higher for MODIS LST (4.63 °C) than North Salve LST data (1.55°C), with MBD of 2.35°C and -0.12°C for MODIS and North Salve LST, respectively.

LST dataset was further compared against MODIS from 2003 to 2021 (ice-covered and open-water separately) for larger study lakes (30 km^2) to avoid pixel mixing with land (Figure 6b). Results showed an RMSD of 2.56°C and MBD of 1.45°C for ice-
315   covered LST, suggesting an overestimation of Landsat-derived LST during this period. On the other hand, an underestimation was observed (MBD = -1.14°C) for open-water LST with a relatively higher RMSD of 3.39. This overestimation was expected as it overestimates LST when compared against in-situ data (Figure 6a). Even though a prior comparison of MODIS LST to surface water temperature demonstrated a lower coefficient of determination, Landsat-derived LST was still further compared against MODIS LST in this study. However, the decision to use MODIS for comparative analysis was due to the unavailability
320   of continuous historical measurements of lake surface temperature. Additionally, MODIS LST provided an added outlook on the capability of Landsat-derived LST to highlight historical trends despite a low temporal resolution by demonstrating a good correlation between the LST values (R = 0.93).
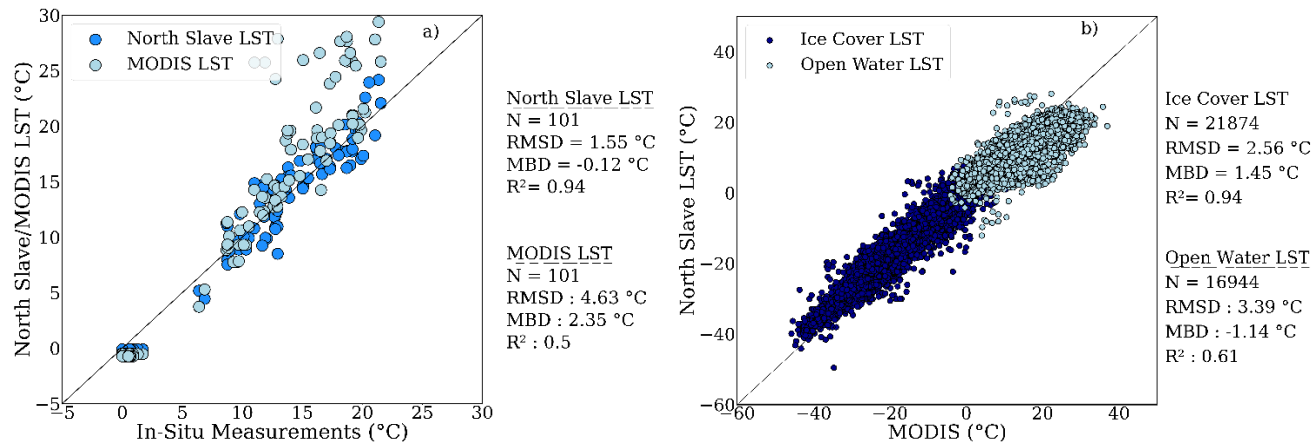
325   **Figure 6: Comparison of North Slave LST and MODIS LST to a) DataStream and ECCC in-situ water surface temperature measurements during open water seasons b) MODIS LST during open water and ice-covered seasons.**

Figures 7a and 7b demonstrate the yearly and monthly RMSD values derived from the comparison between North Slave LST and MODIS LST. Yearly RMSD shows a generally decreasing RMSD from earlier to later years. This may be attributed to Landsat's sensor change in recent years. LST values derived from 2013 onwards were extracted from Landsat-8 OLI/TIRS,

which is known to have improved signal-to-noise ratio and calibration, higher 12-bit radiometric resolution and narrower spectral bands compared to previous sensors (Irons et al., 2012; Roy et al., 2014). Most importantly, Landsat-8 OLI has a radiometric uncertainty of 3% compared to Landsat-7 ETM+ (5%), as well as reduced band saturation (Markham et al., 2014). Monthly RMSD comparing MODIS data to generated LST decreased showed RMSDs were lowest in spring and highest in winter. LST in spring months (March–May) had the lowest RMSD (1.9°C - 2.9°C the least deviation compared with MODIS data.
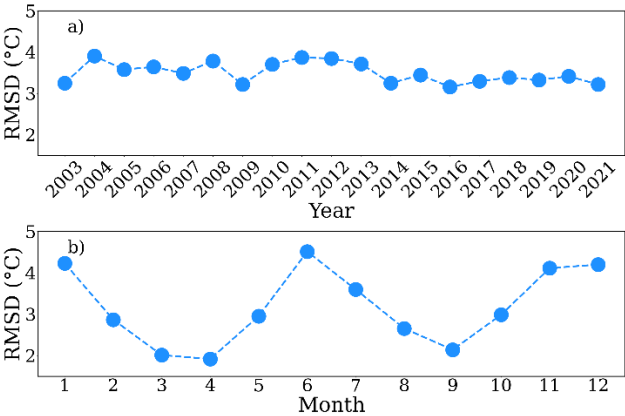
Figure 7: Yearly and monthly RMSD values and mean bias from evaluating North Slave LST against MODIS LST from 2003 to 2021.

4.3 LST Dataset Distribution

4.3.1 Temporal Dataset Distribution of LST Dataset

LST dataset is derived from the thermal radiation of the lakes' uppermost layer, hence the skin temperature. A total of 673,223 gridded data files were included in the generated North Slave LST dataset for the 535 lakes studied across the NSR. The yearly and monthly distribution of the dataset within and between lakes varied temporally, which is highlighted in Figure 8. Overall, the yearly distribution of the North Slave LST dataset was greater in recent years, with the period between 2014 and 2021 having the majority of the data and percentages ranging from 4.15 – 5% of the total dataset. The larger number of data files in recent years was due to LST retrieval from a combination of Landsat-7 and Landsat-8 compared to a single sensor retrieval (Landsat-5) for earlier years. As a result, the highest yearly percentage of the North Slave LST dataset was for 2014 (5%), and the least was for 1988 (1.2%). Most unavailable data for the various years was predominantly because of insufficient usable Landsat data for winter months.

The monthly distribution of the North Slave LST dataset showed the month of May with the highest percentage (13.9%) and December (1.3%) with the lowest. Generally, colder months (October – April) had fewer data (42.7%) compared to relatively warmer months (May – September) (57.3%). Data is unevenly distributed across months and years due to differences in overpass times and influences like cloud cover and other atmospheric impacts on data retrieval.

16

Months

1.4% 2.1% 1.7% 1.3% 1.2% 1.4% 1.3% 1.6% 1.5% 1.6% 1.8% 1.9% 1.7% 1.6% 1.5% 2.2% 1.8% 2.5% 2.5% 3.5% 4.1% 3.3% 3% 2.4% 2.4% 2.7% 2.2% 2.2% 1.4% 3.2% 5% 4.9% 4.5% 4.9% 4.1% 4.4% 4.5% 4.5%

Jan 3.1%

Feb 4.7%

Mar 10.8%

Apr 13.5%

May 13.9%

Jun 12.4%

Jul 12.7%

Aug 10.8%

Sep 7.5%

Oct 5.3%

Nov 4.0%

Dec 1.3%

Years

Number of Images
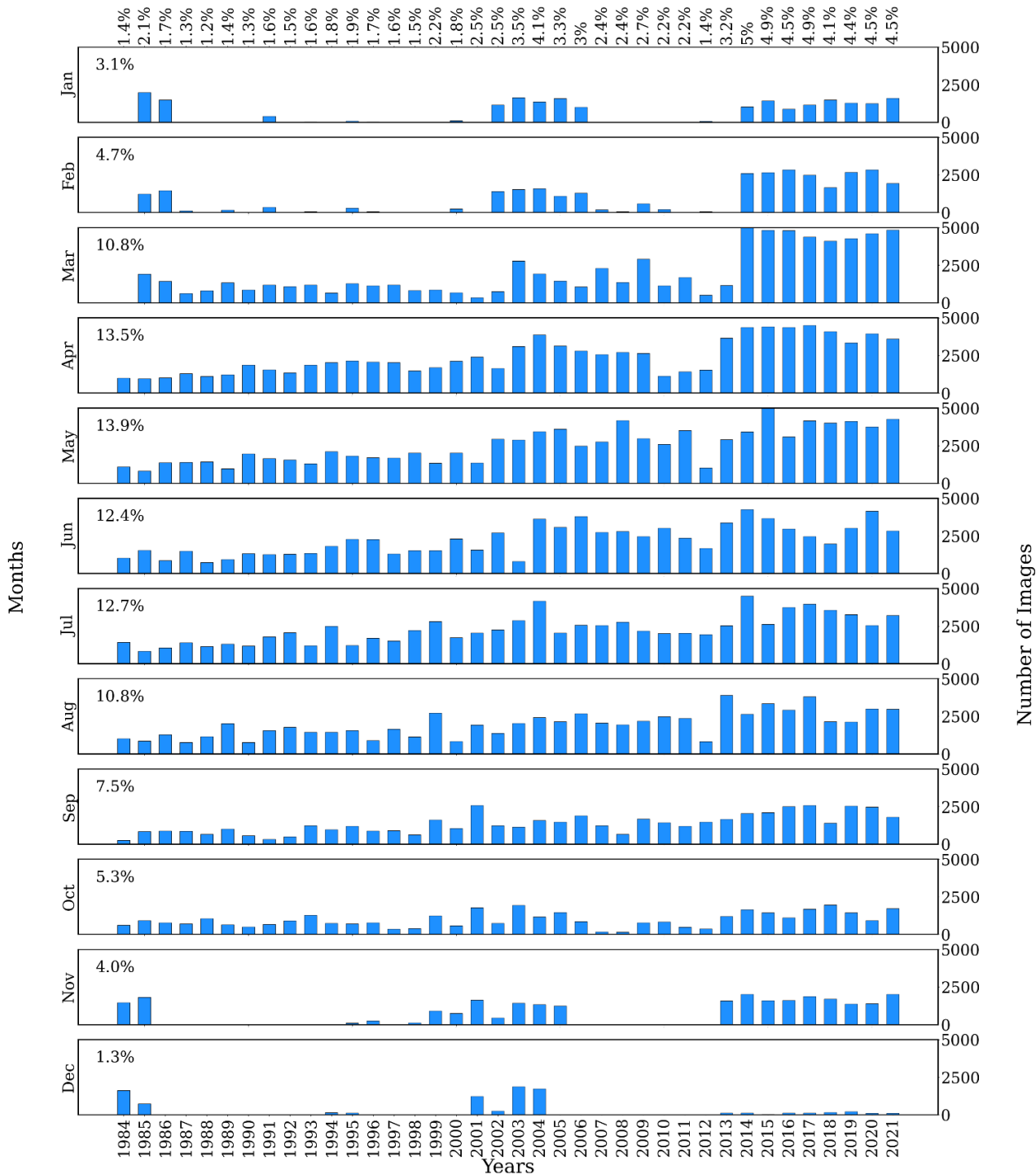
Figure 8: Yearly and monthly distribution of the North Slave LST dataset from 1984 to 2021. Percentages (%) represent the total percentage of the entire data for each month or year.

17

4.3.3 Spatial Dataset Distribution of LST dataset between lakes

While the lakes are widely distributed across the NSR, a large number (144 out of 535) captured in our dataset were within 150 km distance of Yellowknife. The yearly average number of images for each lake in the study region is demonstrated in Figure 9. The average yearly minimum number of images for each lake was 20 and reached a maximum of 45. Lakes with a relatively smaller number of images were mainly distributed around Yellowknife. Smaller-size lakes generally had a smaller number of images compared to relatively larger-sized lakes. This can be attributed mainly to cloud cover covering the entirety of small lakes. The majority of lakes (152 out of 535) had between 40 and 45 images, and 71% of the total lakes in the dataset had more than 30 images per year. Lakes with fewer pixels are more likely to be entirely cloud-covered and lose relatively more surface area due to the lake buffer.
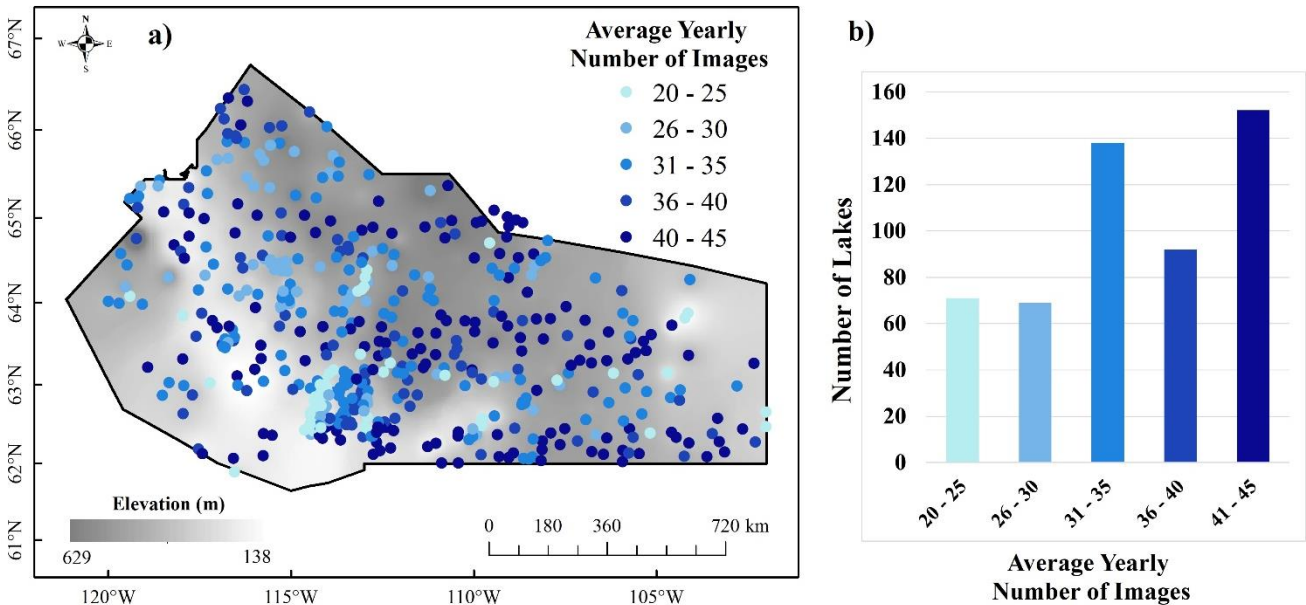
Figure 9: Distribution of the average yearly number of images (available images or useable images) for lakes in the NSR. Can you incorporate lake size somewhere in the right panel here, or would that be too messy?

4.4 North Slave LST dataset

4.4.1 NetCDF Spatial Coverage of LST

The North Slave LST dataset includes LST for 500 lakes with known names and 35 without names. NetCDF (Network Common Data Form) and Tabular data are the data types in this dataset. NetCDF is a file format for storing multidimensional data and hence captures the spatial coverage and dimension of LST for the study lakes in this dataset. To facilitate easy data query, each NetCDF filename includes the name of the lake, date, longitude, latitude, minimum, maximum and mean LST, number of pixels, and the percentage area of the lake LST pixels cover for a given day. The naming convention for lakes and

their explanation is summarised in Table 3. The dataset was grouped based on the name of the lake and further into yearly sub-groups.

The NetCDF files in our dataset have a two-dimensional variable, "lst," which shows the spatial distribution of lake surface temperature. So, in addition, the one-dimensional x and y show the lake's extent and the number of pixels. The spatial reference for the data is the World Geodetic System 1984, EPSG:4326, with a 30-meter resolution.

Table 3: Sections of LST Dataset NetCDF filename and Explanation.

Sample File name: AcastaLake_19840428_ -115.564 _ 65.3783_-5.90_ -7.10_-6.50_17482_099.nc	
Section of Name	**Explanation of the section**
Lake name: AcastaLake	The name of lakes was predominantly derived from the Water file-Lakes and Rivers polygons data from Statistics Canada. Lakes' unknown names were prefixed "NoNameLake" and a number.
Date: 19840428	The date in the NetCDF file is in the format "YYYYMMDD" and represents the date the Landsat scene was captured.
Longitude (°)**:** -115.564	The longitude represents a known longitude predominantly located at the centre of a lake when plotted against the latitude in decimal degrees.
Latitude (°)**:** 65.3783	The latitude represents a known latitude predominantly located at the centre of a lake when plotted against the longitude in decimal degrees.
Maximum temperature (°C)**:** -5.90	This is the maximum LST value retrieved from a lake for a given date which is the coldest part of the lake
Minimum temperature (°C)**:** -7.10	This is the minimum LST value retrieved from a lake for a given date which is the warmest part of the lake
Mean temperature (°C)**:** -6.50	Mean LST value calculated from the number of LST pixels retrieved for a lake on a given date.
Number of LST Pixels: 17482	The number of LST pixels retrieved on a given lake for a given date.
LST pixels coverage (%): **099**	The number of LST pixels retrieved from the lake for a given date is divided by the total number of pixels representing the lake.

4.4.2 Tabular Data of LST

The second type of data included in the dataset is the tabular data with LST statistics on individual study lakes for a given day, including the minimum, maximum, median, number of ice cover pixels, and number of open-water pixels, percentage of lake captured and other lake properties. Table 3 below highlights the column/field names from the tabular data and what they represent. This tabular data is generated for each lake and is included in the dataset. Each filename consists of the lake name followed by longitude and latitude to allow for easy query based on location (e.g., AcastaLake_-115.564 _ 65.3783). Additionally, monthly means were calculated for each lake and combined in one file.

Table 3: Columns names of the tabular dataset and the description.

Column	Description
Lake_Name	Name of the Lake from which the lake surface temperature was retrieved. The name of lakes was predominantly derived from the Water file-Lakes and Rivers polygons data from Statistics Canada. Lakes' unknown names were prefixed "NoNameLake" and a number
Date	The date which the lake surface temperature(LST) represents
Year	The year of the LST in the format "YYYY."
Month	The month of LST in the format "MM."
Day	Day of LST in the format "YY."
Maximum_Temperature	The maximum LST recorded on the lake at a given time in degrees Celcius (°C)
Minimum_Temperature	The maximum LST recorded on the lake at a given time in degrees Celcius (°C)
Median_Temperature	The median LST from all available pixels in degrees Celcius (°C)
Mean_Temperature	The mean LST from all available pixels degrees Celcius (°C)
Total_Pixels	Total number of pixels representing the lake
LST_Pixels	Number of pixels with LST values retrieved from the lake
Percentage_LST_Pixels	Total percentage of pixels with LST values captured from the lake. Values are rounded to the nearest 1
Count_Water_Pixels	Number of LST pixels values greater than 0 retrieved from the lake at a given time
Count_Ice_Pixels	Number of LST pixels values less than 0 retrieved from the lake at a given time
Percentage_Ice_Pixels	Total percentage of ice pixels captured from the lake at a given time. Values are rounded to the nearest 1.
Landsat_Row_Path	Tile name, Row and path of the Landsat from which LST was retrieved
Lake_Area	Surface Area of the Lake in square kilometres (km^2)
HyLak_ID	The ID is derived from the HydroLAKES dataset. Lakes with no ID are indicated with 0.
HyLak_Depth	The average depth of the lake derived from the HydroLAKES dataset in meters (m)
HyLak_Volume	The volume of the lake derived from the HydroLAKES dataset is million cubic meters (1 mcm = 0.001km^3)
HyLak_Elevation	Elevation of the lake surface derived from HydroLAKES dataset in meters above sea level
Long(m)	Longitude point on the lake in meters
Lat(m)	Latitude point on the lake in meters
Long(DD)	Longitude point on the lake in decimal degrees
Lat(DD)	Latitude point on the lake in decimal degrees
Monthly_Mean_Temperature	The mean LST on the lake for a given month

4.5 Spatial Patterns of North Slave LST

4.5.1 Seasonal Lake Spatial Distribution of North Slave LST

The seasonal spatial distribution of mean LST from 1984 to 2021 is shown in Figure 10 to highlight the spatial variation of LST for different seasons. The distribution of average LST was computed for winter (December - January), spring (March-

May), summer (June – August) and autumn (September – November) for all study lakes. LST on lakes in the NSR is generally
negative in winter (-26 – -18°C) and spring (-17 – -3). This is because lakes are ice-covered during these two seasons,
constituting negative LST values. Autumn was characterised by both positive and negative LST values (-8 – 3°C). Lakes start
to freeze in autumn, and the freezing rate is influenced by several factors resulting in differences in the open-water duration,
which affect average temperature. The average LST for summer values ranged from 6 - 22°C. Average LST ranges between
lakes were the lowest in the winter (Figure 10a), with a variability of 8 °C. However, the largest LST variability between lakes
for summer was twice that of winter (16°C). This is expected as temperatures on lakes during this season are influenced by
several factors, including lake size, elevation, depth, latitude, longitude and volume (O'Reilly et al., 2015; Xie et al., 2022) in
addition to air temperature. Seasonal LST spatial distribution provides insight into the climate patterns of the NSR region.

Figure 10: Spatial distribution of average LST across the NSR showing taken across all years for a) winter, b) spring, c) summer and d) autumn.

21

4.5.2 Spatial Distribution of LST for 2021

The spatial distribution of the mean annual LST across the NSR for 2021 is shown in Figure 11a, which highlights remarkable spatial differences between lakes at higher versus lower elevations, with lower-elevation lakes generally demonstrating higher LST. Based on the mean annual LST values in 2021, the LST category was divided into five different ranges, as shown in the map [-12 -9°C, -9 - -6°C, -6 - -3°C, -3 - 0°C, and 0 - 3°C]. Figure 11 b shows most lakes (28%) with a mean of -3 - 0. Lake distribution of mean temperature was 8%, 22%, 27%, 28% and 15% from colder to warmer LST categories, respectively. The percentage of the total area covered by lakes in relation to mean LST was 34%, 27%, 18%, 19% and 2%, respectively (Figure 11b). Although the number of lakes with LST ranging from -12 -9°C was the least (8% of lakes), the percentage of the total area covered by lakes with this LST range was the largest (34% of lakes). The total area covered for all lakes with mean LST from 0 - 3°C was only 2%. This suggests that several of the lakes with warmer temperatures were smaller in size. Generally, relatively warmer lakes were also distributed around Yellowknife and the southwestern part of the region.
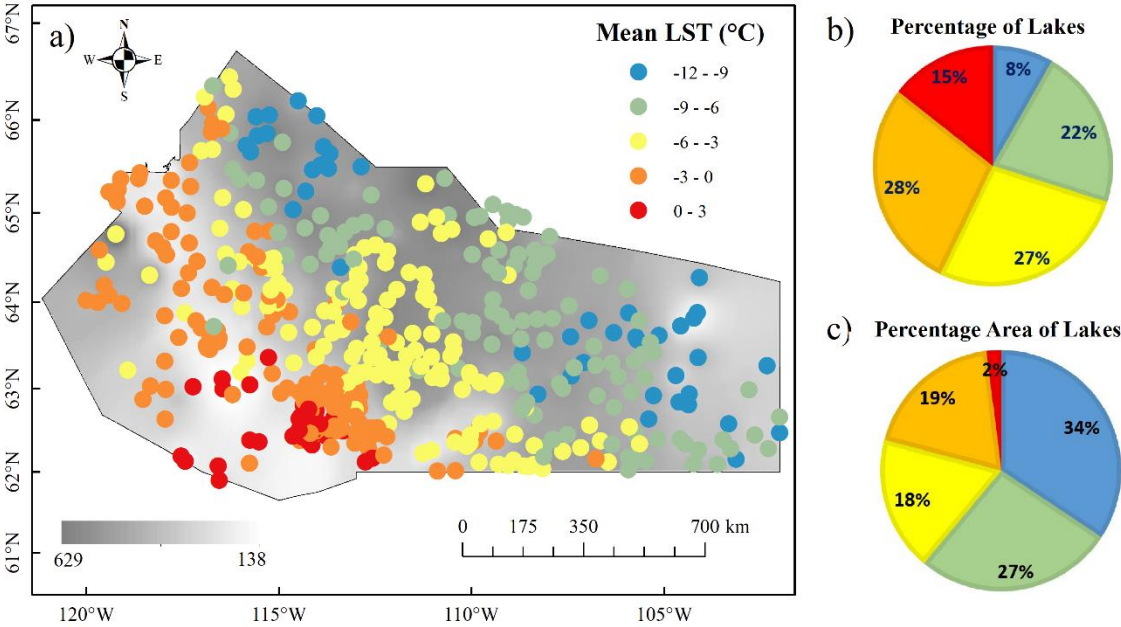
Figure 11: Spatial distribution of mean LST for the year 2021 across the NSR showing b) the percentage number of lakes and c) the percentage area of lakes within specific LST ranges.

4.5.3 Intra-Lake Spatial Distribution of generated LST

Lakes in several studies are treated as homogenous entities; however, for a given lake, there is spatial variability in the surface temperature based on several factors, including the difference in morphometry or biological, physical, and anthropogenic activities occurring on the lake at a given time (Crosman & Horel, 2009; Huang et al., 2017; Selman & Misra, 2014; Yang et al., 2020). In view of this, the North Slave LST datasets generated in this study can highlight the spatial variability within a given lake. As expected, the high spatial resolution and multidate LST generated show lakes' surface temperature

22

heterogeneity. The phenomenon is demonstrated with LST on July 9 2021, for a few selected lakes within our study as examples (Figure 12).

Lakes may demonstrate significant surface temperature variations for various reasons, including wind redistribution, depth, and biological and anthropogenic activities. Warmer LSTs are generally at the shallower coastal regions of lakes; however, internal LST variations differ. An example is in the case of Lake Duncan (Figure 12), which demonstrated warmer temperatures in the north part of the lake than in the south. Maximum and minimum LST on lakes also differ, with some lakes having wider variations (*e.g*., Duncan Lake (23 – 14°C) and Frame Lake (28 – 24°C)). Lakes' physical differences, location and elevation may contribute to the different ranges of surface temperature distribution on individual lakes.
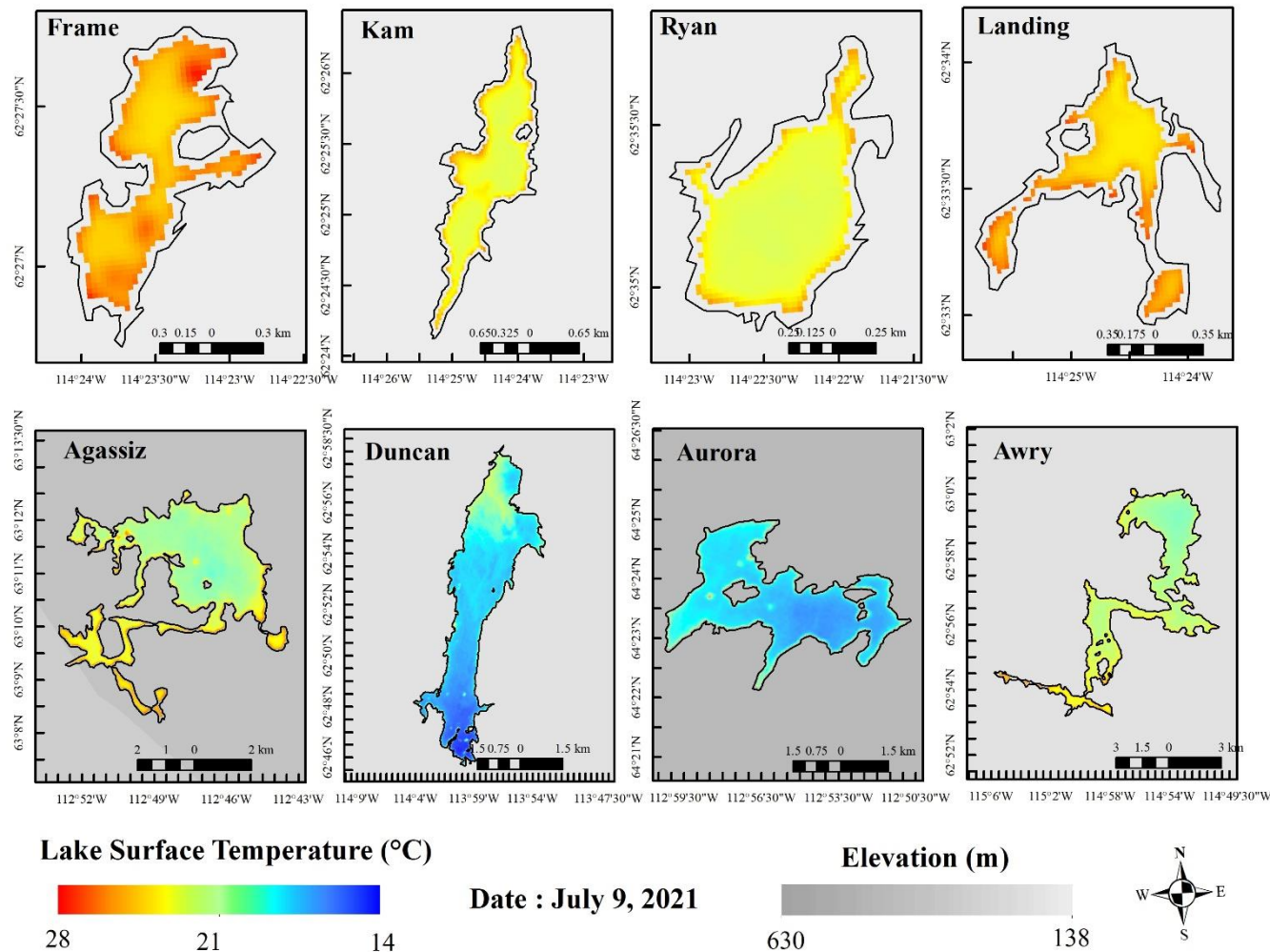
Figure 12: Intra-lake spatial distribution of LST on selected lakes in the NSR highlighting the dataset's ability to capture small-scale details of LST.

23

5 Data availability

The long-term (1984 -2021) continuous high-resolution (30 m spatial resolution) regional (North Slave region, NWT) gridded LST dataset is available at https://doi.org/10.5683/SP3/J4GMC2 (Attiah et al., 2022) and the Government of Northwest Territories (NWT) Discovery Portal (DOI will be made available at the end of the publication process). Additional data used in this study include the Landsat imagery can be downloaded from the USGS platform. Physical properties and names of lakes were derived from HydroLAKES (https://www.hydrosheds.org/products/hydrolakes), Water file-Lakes and Rivers polygons data (https://www12.statcan.gc.ca/census-recensement/2011/geo/bound-limit/files-fichiers/ghy_000c06a_e.zip) and CanVec series (https://open.canada.ca/data/en/dataset/9d96e8c9-22fe-4ad2-b5e8-94a6991b744b). Evaluation data was derived from Mackenzie DataStream (https://mackenziedatastream.ca/). ERA5 reanalysis data was obtained from Copernicus Climate Change Service (https://cds.climate.copernicus.eu/#!/search?text=ERA5&type=dataset).

6 Conclusions

A new gridded dataset (North Slave LST) of lake surface temperature across the NSR, NWT was presented in this study based on an LST retrieval algorithm adapted to the thermal bands of Landsat archives. LST data is available for 38 years (from 1984 to 2021) on a 30 m spatial resolution with varying temporal resolution (minimum of 1 day). North Slave LST dataset has proven comparable with LST products like MODIS (1 km resolution) and other water surface temperature measurements that it is suitable for capturing small-scale details of LST on small lakes.

The North Slave LST dataset includes 673,223 NetCDF gridded data files for all lakes, with a greater percentage (57.3%) highlighting LST in warmer months. A high percentage (43%) of the dataset was derived from Landsat-5. Lakes had a 100-meter buffer applied, resulting in a pixel representing 16.7% to 97.34% of the lake area. Most of the dataset (77.4%) had LST pixels coverage greater than 50%, of which 42.2% had pixels coverage greater than 90%. The average yearly number of LST files for each lake was between 20 and 45.

The retrieval algorithm successfully retrieves LST from Landsat images across the NSR with an RMSD of 1.7°C and MBD of 0.12. The dataset produced provides continuous data and highlights spatial and temporal LST of lakes in the NSR. Based on generated North Slave LST, warmer lakes are predominantly located around the town of Yellowknife and on the southwestern part of the NSR. Seasonal average LST is also highlighted using generated LST, with summer having the highest variation of LST (16°C) between lakes. Intra-lake variability is also heightened with this dataset. The North Slave LST dataset will be continually updated with improved retrieval algorithms and up-to-date data as they become available.

24

Author Contributions

Gifty Attiah – Methodology, Analysis, Writing and sVisualisation – original draft.
Homa Kheyrollah Pour – Supervision, Resources, Writing – review & editing
Andrea Scott - Supervision, Resources, Writing – review & editing

Competing Interests

The authors declare no competing interest.

References

Attiah, G., Kheyrollah Pour, K., & Scott, K. A. (2022). North Slave Lake Surface Temperature Retrieved from Landsat Archives from 1984 to 2021. https://doi.org/10.5683/SP3/J4GMC2

Austin, J. A., & Colman, S. M. (2007). Lake Superior summer water temperatures are increasing more rapidly than regional temperatures: A positive ice-albedo feedback. *Geophysical Research Letters*, *34*(6), 1–5. https://doi.org/10.1029/2006GL029021

Chander, G., & Markham, B. (2003). Revised Landsat-5 TM Radiometric Calibration Procedures and Postcalibration Dynamic Ranges. *IEEE Transactions on Geoscience and Remote Sensing*, *41*(11 PART II), 2674–2677. https://doi.org/10.1109/TGRS.2003.818464

Chen, Y., Zhao, C., & Ming, Y. (2019). Potential impacts of Arctic warming on Northern Hemisphere mid-latitude aerosol optical depth. In *Climate Dynamics* (Vol. 53, Issues 3–4, pp. 1637–1651). https://doi.org/10.1007/s00382-019-04706-3

Collingsworth, P. D., Bunnell, D. B., Murray, M. W., Kao, Y. C., Feiner, Z. S., Claramunt, R. M., Lofgren, B. M., Höök, T. O., & Ludsin, S. A. (2017). Climate change as a long-term stressor for the fisheries of the Laurentian Great Lakes of North America. *Reviews in Fish Biology and Fisheries*, *27*(2), 363–391. https://doi.org/10.1007/s11160-017-9480-3

Crosman, E. T., & Horel, J. D. (2009). Remote Sensing of Environment MODIS-derived surface temperature of the Great Salt Lake. *Remote Sensing of Environment*, *113*(1), 73–81. https://doi.org/10.1016/j.rse.2008.08.013

Desai, A. R., Austin, J. A., Bennington, V., & McKinley, G. A. (2009). Stronger winds over a large lake in response to weakening air-to-lake temperature gradient. *Nature Geoscience*, *2*(12), 855–858. https://doi.org/10.1038/ngeo693

495   Eerola, K., Rontu, L., Kourzeneva, E., Kheyrollah Pour, H., Duguay, C. R. (2014). Impact of partly ice-free Lake Ladoga on temperature and cloudiness in an anticycl*onic winter situation–a case study using a limited area model. Tellus A: Dynamic Meteorology and Oceanography 66 (1), 23929. DOI: 10.3402/tellusa.v66.23929*

500   Environment and Climate Change Canada, Université de Montréal. 2020-07-11. "CIMP 161_Legacy arsenic pollution in Yellowknife Bay sediments" (dataset). 1.0.0. DataStream. https://doi.org/10.25976/gm49-2a19.

Fichot, C. G., Matsumoto, K., Holt, B., Gierach, M. M., & Tokos, K. S. (2019). Assessing change in the overturning behavior of the Laurentian Great Lakes using remotely sensed lake surface water temperatures. *Remote Sensing of Environment*, *235*(October), 111427. https://doi.org/10.1016/j.rse.2019.111427

505   Hersbach, H., Bell, B., Berrisford, P., Hirahara, S., Horányi, A., Muñoz-Sabater, J., Nicolas, J., Peubey, C., Radu, R., Schepers, D., Simmons, A., Soci, C., Abdalla, S., Abellan, X., Balsamo, G., Bechtold, P., Biavati, G., Bidlot, J., Bonavita, M., … Thépaut, J.-N. (2020). The ERA5 global reanalysis. *Q J R Meteorol Soc*, *146*, 1999–2049. https://doi.org/10.1002/qj.3803

Huang, Y., Liu, H., Hinkel, K., Yu, B., Beck, R., & Wu, J. (2017). Analysis of Thermal Structure of Arctic Lakes at Local and 510   Regional Scales Using in Situ and Multidate Landsat-8 Data. *Water Resources Research*, *53*(11), 9642–9658. https://doi.org/10.1002/2017WR021335

Ihlen, V., & Zanter, K. (2019). Landsat 7 (L7) Data Users Handbook. *USGS Landsat User Services*, *7*(November), 151.

Irons, J. R., Dwyer, J. L., & Barsi, J. A. (2012). The next Landsat satellite: The Landsat Data Continuity Mission. *Remote Sensing of Environment*, *122*, 11–21. https://doi.org/10.1016/j.rse.2011.08.026

515   Jimenez-Munoz, J. C., Cristobal, J., Sobrino, J. A., Sòria, G., Ninyerola, M., & Pons, X. (2009). Revision of the single-channel algorithm for land surface temperature retrieval from landsat thermal-infrared data. *IEEE Transactions on Geoscience and Remote Sensing*, *47*(1), 339–349. https://doi.org/10.1109/TGRS.2008.2007125

Jiménez-Munoz, J. C., & Sobrino, J. A. (2003). A generalized single-channel method for retrieving land surface temperature from remote sensing data. *Journal of Geophysical Research: Atmospheres*, *108*(22). 520   https://doi.org/10.1029/2003jd003480

Jimenez-Munoz, J. C., Sobrino, J. A., Skokovic, D., Mattar, C., & Cristobal, J. (2014). Land surface temperature retrieval methods from landsat-8 thermal infrared sensor data. *IEEE Geoscience and Remote Sensing Letters*, *11*(10), 1840–1843. https://doi.org/10.1109/LGRS.2014.2312032.

Kheyrollah Pour, H., Duguay, C. R., Martynov, A., & Brown, L. C. (2012). Simulation of surface temperature and ice cover 525   of large northern lakes with 1-D models: A comparison with MODIS satellite data and in situ measurements. *Tellus, Series A: Dynamic Meteorology and Oceanography*, *64*(1). https://doi.org/10.3402/tellusa.v64i0.17614

Kheyrollah Pour, H., Duguay, C. R., Scott, K. A., & Kang, K. K. (2017). Improvement of Lake Ice Thickness Retrieval from MODIS Satellite Data Using a Thermodynamic Model. *IEEE Transactions on Geoscience and Remote Sensing*, *55*(10),

5956–5965. https://doi.org/10.1109/TGRS.2017.2718533

530   Kheyrollah Pour, H., Duguay, C., Solberg, R., & Rudjord, Ø. (2014a). Impact of satellite-based lake surface observations on the initial state of HIRLAM. Part I: evaluation of remotely-sensed lake surface water temperature observations. *Tellus A: Dynamic Meteorology and Oceanography*, *66*(1), 21534. DOI: 10.3402/tellusa.v66.21534

Kheyrollah Pour, H., Rontu, L., Duguay, C., Eerola, K., & Kourzeneva, E. (2014b). Impact of satellite-based lake surface observations on the initial state of HIRLAM. Part II: Analysis of lake surface temperature and ice cover. *Tellus A: Dynamic Meteorology and Oceanography*, *66*(1), 21395. https://doi.org/10.3402/tellusa.v66.21395

535

Kraemer, B. M., Anneville, O., Chandra, S., Dix, M., Kuusisto, E., Livingstone, D. M., Rimmer, A., Schladow, S. G., Silow, E., Sitoki, L. M., Tamatamah, R., Vadeboncoeur, Y., & McIntyre, P. B. (2015). Strati Fi Cation Responses To Climate Change. *Geophysical Research Letters*, *42*, 4981–4988. https://doi.org/10.1002/2015GL064097

Livingstone, D. M., Lotter, F., & Kettle, H. (2005). *Altitude-dependent differences in the primary physical response of mountain lakes to climatic forcing*. *50*(4), 1313–1325.

540

Magnuson, J. J., Robertson, D. M., Benson, B. J., Wynne, R. H., Livingstone, D. M., Arai, T., Assel, R. A., Barry, R. G., Card, V., Kuusisto, E., Granin, N. G., Prowse, T. D., Stewart, K. M., & Vuglinski, V. S. (2000). Historical trends in lake and river ice cover in the Northern Hemisphere. *Science*, *289*(5485), 1743–1746. https://doi.org/10.1126/science.289.5485.1743

545   Markham, B., Barsi, J., Kvaran, G., Ong, L., Kaita, E., Biggar, S., Czapla-Myers, J., Mishra, N., & Helder, D. (2014). Landsat-8 operational land imager radiometric calibration and stability. In *Remote Sensing* (Vol. 6, Issue 12, pp. 12275–12308). https://doi.org/10.3390/rs61212275

Merchant, C. J., Paul, F., Popp, T., Ablain, M., Bontemps, S., Defourny, P., Hollmann, R., Lavergne, T., Laeng, A., De Leeuw, G., Mittaz, J., Poulsen, C., Povey, A. C., Reuter, M., Sathyendranath, S., Sandven, S., Sofieva, V. F., & Wagner, W.

550   (2017). Uncertainty information in climate data records from Earth observation. *Earth System Science Data*, *9*(2), 511–527. https://doi.org/10.5194/essd-9-511-2017

Messager, M. L., Lehner, B., Grill, G., Nedeva, I., & Schmitt, O. (2016). Estimating the volume and age of water stored in global lakes using a geo-statistical approach. *Nature Communications*, *7*, 1–11. https://doi.org/10.1038/ncomms13603

Moigne, P. Le, Colin, J., & Decharme, B. (2016). *Tellus A : Dynamic Meteorology and Oceanography Impact of lake surface*

555   *temperatures simulated by the FLake scheme in the CNRM-CM5 climate model Impact of lake surface temperatures simulated by the FLake scheme in the CNRM-CM5 climate model. 0870*. https://doi.org/10.3402/tellusa.v68.31274

O'Reilly, C. M., Rowley, R. J., Schneider, P., Lenters, J. D., Mcintyre, P. B., & Kraemer, B. M. (2015). Rapid and highly variable warming of lake surface waters around the globe. Geophysical Research Letters, 42: 1-9. *Geophysical Research Letters*, 1–9. https://doi.org/10.1002/2015GL066235.Received

560   Pekel, J. F., Cottam, A., Gorelick, N., & Belward, A. S. (2016). High-resolution mapping of global surface water and its long-term changes. *Nature*, *540*(7633), 418–422. https://doi.org/10.1038/nature20584

Prats, J., Reynaud, N., Rebière, D., Peroux, T., Tormos, T., & Danis, P.-A. (2018). LakeSST: Lake Skin Surface Temperature

in French inland water bodies for 1999–2016 from Landsat archives. *Earth System Science Data*, *10*(2), 727–743. https://doi.org/10.5194/essd-10-727-2018

565 Reinart, A., & Reinhold, M. (2008). *Mapping surface temperature in large lakes with MODIS data*. *112*, 603–611. https://doi.org/10.1016/j.rse.2007.05.015

Roy, D. P., Wulder, M. A., Loveland, T. R., C.E., W., Allen, R. G., Anderson, M. C., Helder, D., Irons, J. R., Johnson, D. M., Kennedy, R., Scambos, T. A., Schaaf, C. B., Schott, J. R., Sheng, Y., Vermote, E. F., Belward, A. S., Bindschadler, R., Cohen, W. B., Gao, F., … Zhu, Z. (2014). Landsat-8: Science and product vision for terrestrial global change research.

570 *Remote Sensing of Environment*, *145*, 154–172. https://doi.org/10.1016/j.rse.2014.02.001

Schneider, P., & Hook, S. J. (2010). Space observations of inland water bodies show rapid surface warming since 1985. *Geophysical Research Letters*, *37*(22), 1–5. https://doi.org/10.1029/2010GL045059

Selman, C., & Misra, V. (2014). Journal of Geophysical Research : Atmospheres. *Journal of Geophysical Research*, *3*, 180–198. https://doi.org/10.1002/2013JD021040.Received

575 Sentlinger, G. I., Hook, S. J., & Laval, B. (2008). Sub-pixel water temperature estimation from thermal-infrared imagery using vectorized lake features. *Remote Sensing of Environment*, *112*(4), 1678–1688. https://doi.org/10.1016/j.rse.2007.08.019

Shi, Q., & Xie, P. (2019). *Impact of Lake Surface Temperature Variations on Lake Effect Snow Over the Great Lakes Region Journal of Geophysical Research : Atmospheres*. *1999*, 553–567. https://doi.org/10.1029/2019JD031261

Sima, S., Ahmadalipour, A., & Tajrishy, M. (2013). Mapping surface temperature in a hyper-saline lake and investigating the

580 effect of temperature distribution on the lake evaporation. *Remote Sensing of Environment*, *136*, 374–385. https://doi.org/10.1016/j.rse.2013.05.014

Slater, J. A., Garvey, G., Johnston, C., Haase, J., Heady, B., Kroenung, G., & Little, J. (2006). The SRTM data "finishing" process and products. *Photogrammetric Engineering and Remote Sensing*, *72*(3), 237–247. https://doi.org/10.14358/PERS.72.3.237

585 U.S. Geological Survey. (2016). Landsat 8 Data Users Handbook. *Nasa*, *8*(June), 97. https://landsat.usgs.gov/documents/Landsat8DataUsersHandbook.pdf

U.S. Geological Survey. (2022). Landsat Level-1 Processing Details, accessed March 11, 2022, at URL: https://www.usgs.gov/landsat-missions/landsat-level-1-processing-details

Wan, Z., Zhang, Y., Zhang, Q., & Li, Z. liang. (2002). Validation of the land-surface temperature products retrieved from terra

590 moderate resolution imaging spectroradiometer data. *Remote Sensing of Environment*, *83*(1–2), 163–180. https://doi.org/10.1016/S0034-4257(02)00093-7

Wang, J., Xue, P., Pringle, W., Yang, Z., & Qian, Y. (2021). *Impacts of Lake Surface Temperature on the Summer Climate Over the Great Lakes Region Journal of Geophysical Research : Atmospheres*. 1–20. https://doi.org/10.1029/2021JD036231

595 Wloczyk, C., Richter, R., Borg, E., & Neubert, W. (2006). Sea and lake surface temperature retrieval from Landsat thermal data in Northern Germany. In *International Journal of Remote Sensing* (Vol. 27, Issue 12, pp. 2489–2502).

https://doi.org/10.1080/01431160500300206

Woolway, R. I., Kraemer, B. M., Lenters, J. D., Merchant, C. J., O'Reilly, C. M., & Sharma, S. (2020). Global lake responses to climate change. *Nature Reviews Earth and Environment*, *1*(8), 388–403. https://doi.org/10.1038/s43017-020-0067-5

Woolway, R. I., Merchant, C. J., Van Den Hoek, J., Azorin-Molina, C., Nõges, P., Laas, A., Mackay, E. B., & Jones, I. D. (2019). Northern Hemisphere Atmospheric Stilling Accelerates Lake Thermal Responses to a Warming World. *Geophysical Research Letters*, *46*(21), 11983–11992. https://doi.org/10.1029/2019GL082752

Xie, C., Zhang, X., Zhuang, L., Zhu, R., & Guo, J. (2022). Analysis of surface temperature variation of lakes in China using MODIS land surface temperature data. In *Scientific Reports* (Vol. 12, Issue 1). https://doi.org/10.1038/s41598-022-06363-9

Yang, K., Yu, Z., & Luo, Y. (2020). Analysis on driving factors of lake surface water temperature for major lakes in Yunnan-Guizhou Plateau. *Water Research*, *184*, 116018. https://doi.org/10.1016/j.watres.2020.116018

Young, N. E., Anderson, R. S., Chignell, S. M., Vorster, A. G., Lawrence, R., & Evangelista, P. H. (2017). A survival guide to Landsat preprocessing. *Ecology*, *98*(4), 920–932. https://doi.org/10.1002/ecy.1730

Zhang, G., Yao, T., Chen, W., Zheng, G., Shum, C. K., Yang, K., Piao, S., Sheng, Y., Yi, S., Li, J., O'Reilly, C. M., Qi, S., Shen, S. S. P., Zhang, H., & Jia, Y. (2019). Regional differences of lake evolution across China during 1960s–2015 and its natural and anthropogenic causes. *Remote Sensing of Environment*, *221*(November 2018), 386–404. https://doi.org/10.1016/j.rse.2018.11.038

Zhang, X., Duan, K. qin, Shi, P. hong, & Yang, J. hua. (2016). Effect of lake surface temperature on the summer precipitation over the Tibetan Plateau. *Journal of Mountain Science*, *13*(5), 802–810. https://doi.org/10.1007/s11629-015-3743-z

Zhao, G., Gao, H., & Cai, X. (2020). Estimating lake temperature profile and evaporation losses by leveraging MODIS LST data. *Remote Sensing of Environment*, *251*(May), 112104. https://doi.org/10.1016/j.rse.2020.112104

Appendices

Appendix A

Lake name	Latitude (°)	Longitude (°)	Area(km²)	Elevation (m)	Average Depth (m)	Number of Pixels	Percentage of lake represented
Acasta Lake	-115.564	65.3783	18.23	399	4.7	17645	87.11
Achilles Lake	-110.906	64.963	27.84	403	16.7	27536	89.01
Acres Lake	-108.688	62.7499	3.36	333	9.6	2438	65.18
Agassiz Lake	-112.788	63.1797	19.89	338	17.9	18113	81.95
Ajax Lake	-110.58	64.9737	24.32	446	8.2	23524	87.05
Alexander Lake	-108.117	62.2884	6.24	385	6.8	5427	78.21
Alexie Lake	-114.083	62.6779	4.24	218	6	3357	71.23
Allan Lake	-113.063	62.9208	4.35	273	8	3893	80.46
Ambush Lake	-113.824	65.7125	16.02	413	13.6	15379	86.39
Angelique Lake	-113.421	64.6265	17.84	403	10.2	16742	84.47

Angle Lake	-114.177	62.8313	4.11	195	21.1	3404	74.45
Anton Lake	-114.461	62.9713	3.34	253	8.8	2404	64.67
Ardent Lake	-115.736	65.6577	14.28	412	6.2	14331	90.34
Armi Lake	-114.124	63.7112	26.59	354	9.6	25165	85.18
Arno Lake	-113.533	63.0506	0.11	-	-	43	36.36
Artillery Lake	-107.871	63.1744	521.89	352	24.3	552430	95.27
Athenia Lake	-111.516	63.6452	42.29	416	7.2	38069	81.01
Augustus Lake	-116.686	66.3619	9.78	340	22.3	9027	83.03
Aurora Lake	-112.921	64.3918	15.25	377	5.3	14892	87.8
Awry Lake	-114.922	62.9506	26.89	201	19.7	25545	85.5
Axecut Lake	-104.138	63.8762	1.95	165	5.6	1789	82.56
Aylmer Lake	-108.53	64.1244	680.73	355	19.7	715690	94.62
Back Lake	-109.329	63.8188	86.59	384	12.9	87319	90.76
Back River	-108.275	64.609	62.66	333	15.6	61472	88.29
Baldhead Lake	-113.634	64.6092	20.02	409	11.2	19439	87.41
Banting Lake	-114.285	62.6292	3.86	171	10.9	2959	68.91
Barnston Lake	-110.033	63.1483	12.64	384	15	11950	85.13
Bartlett Lake	-118.336	63.0863	183.8	260	4.4	191259	93.65
Basile Lake	-111.261	62.2174	15.19	171	20.2	15196	90.06
Basler Lake	-115.945	63.9303	99.21	230	40.3	99610	90.36
Baton Lake	-115.096	64.3761	1.83	327	11.8	1089	53.55
Bear Lake	-114.184	62.3801	1.7	173	3.9	1158	61.18
Beauparlant Lake	-112.177	64.5722	13.62	445	6.6	12519	82.75
Beauregard Lake	-114.336	62.7216	1.46	207	7.6	1220	75.34
Beaverhill Lake	-104.373	62.8032	121.51	278	12.9	129356	95.81
Beaverlodge Lake	-118.194	64.6873	65.31	175	6.7	64188	88.46
Beck Lake	-104.613	62.8365	4.82	282	1.8	4839	90.46
Bedford Lake	-109.496	62.9993	25.91	306	15.8	23905	82.86
Bell Lake	-114.334	62.8427	3.82	226	7.1	3104	73.04
Benoit Lake	-116.251	66.3525	25.65	379	6.6	24857	87.21
Bessonette Lake	-114.741	63.6612	8.57	296	10.2	7970	83.66
Betty Ray Lake	-116.574	63.5419	6.07	196	6.1	4935	73.15
Bewick Lake	-105.718	62.4994	85.96	341	8.4	83936	87.88
Big Lake	-112.986	64.857	65.63	407	7.8	66426	91.09
Big Rocky Lake	-102.294	62.2768	78.01	254	8.1	75539	87.16
Bighill Lake	-114.036	62.5076	4.58	189	6.2	4342	85.37
Biologist Lake	-104.087	64.2761	3.48	300	2.5	3336	86.21
Birch Lake	-116.565	62.067	85.93	187	5.7	89784	94.04
Bishop Lake	-116.157	65.5005	46.4	347	14.8	47643	92.41
Black Lichen Lake	-116.263	64.4217	58.82	287	23.7	58221	89.07
Blaisdell Lake	-113.579	62.7784	5.95	249	6.6	5191	78.49
Blake Lake	-106.448	62.1172	12.76	389	5.3	11905	83.93
Bodie Lake	-105.853	62.9572	14.88	341	5.6	14557	88.04
Boland Lake	-115.69	64.5396	28.93	255	33.6	26869	83.44
Boulder Lake	-113.074	63.7656	16.91	361	13.2	16609	88.35
Box Lake	-109.423	63.9199	39.37	384	12.9	38395	87.78
Bras dOr Lake	-115.743	62.3927	33.03	-	-	34349	93.58
Breadner Lake	-116.749	65.8623	27.34	295	19.7	27433	90.31
Breithaupt Lake	-105.407	62.6386	19.67	335	2.9	18063	82.66
Bridge Lake	-112.276	63.268	3.58	395	6.9	3013	75.7
Brock Lake	-112.833	62.4155	0.17	255	3.1	81	41.18
Broken Dish Lake	-116.267	65.8579	3.91	368	11.9	3721	85.68
Brown Water Lake	-115.863	64.5998	51.97	275	35	45575	78.7
Buckham Lake	-112.647	62.2974	30.98	189	19.6	28839	83.8
Bunting Lake	-109.783	62.4827	0.23	235	2.9	167	65.22
Burbanks Lake	-108.6	62.7652	0.08	-	-	37	37.5
Burke Lake	-116.712	63.5178	2.37	170	7.9	2074	78.9
Bustard Lake	-108.415	64.3342	7.41	372	10.8	7067	85.83
Calder Lake	-115.234	65.8658	15.31	454	6.8	14620	85.83
Calypso Lake	-115.844	65.7256	12.98	380	12.4	11701	81.12
Campbell Lake	-106.894	63.2391	110.9	373	7.8	105646	85.73
Camsell Lake	-111.185	63.6228	158.16	411	12.6	153622	87.42
Carey	-102.909	62.2067	255.34	265	12.1	259064	91.24
Caribou Lake	-114.023	62.986	2.78	245	4.9	2077	67.27

Carter Lake	-104.303	62.9554	29.59	274	8.1	27590	83.91
Cassino Lake	-119.398	64.0755	22.44	325	4.4	23561	94.47
Castor Lake	-115.978	64.4679	35.74	284	28.6	34101	85.87
Chan 1 Lake	-114.355	62.6408	0.41	236	2.8	238	51.22
Chan Lake	-116.542	61.8909	0.84	239	6.5	701	75
Chartrand Lake	-115.532	64.4607	20.79	336	16.7	19626	84.94
Chedabucto Lake	-115.553	62.3691	43.01	193	5.7	44908	93.98
Chelay Lake	-119.403	65.2223	1.72	199	5.6	1393	72.67
Chipp Lake	-112.626	62.4685	2.9	270	2.1	2056	63.79
Chitty Lake	-114.123	62.7149	2.38	221	6.2	1822	68.91
Clinton Colden Lake	-107.474	63.9586	599.71	352	13.4	608092	91.23
Clive Lake	-118.906	63.212	64.84	255	3.6	66713	92.47
Coldblow Lake	-104.107	63.361	12.1	320	3.8	11726	87.19
Cole Lake	-116.594	63.6731	9.24	194	11.9	8010	77.92
Compton Lake	-109.79	62.5331	8.91	246	26.2	9010	91.02
Consolation Lake	-112.797	62.5081	20.01	238	14.8	15423	69.37
Contwoyto Lake	-110.506	65.3085	163.62	435	22.2	166125	91.38
Cook Lake	-108.849	63.1595	49.99	352	10.2	45458	81.84
Cooley Lake	-109.052	62.0574	9.33	336	10	8220	79.31
Cosmos Lake	-104.224	63.8148	2.14	150	8.9	2052	85.98
Cotterill Lake	-114.847	64.1539	17.93	334	10.9	16688	83.77
Courageous Lake	-111.188	64.1657	228.32	395	12.6	232082	91.48
Courier Lake	-111.946	63.5337	1.46	439	3.8	1092	67.12
Cowan Lake	-115.274	63.3612	4.44	218	9.7	3373	68.47
Crapaud Lake	-114.021	62.9358	5.87	225	5.3	4945	75.81
Credit Lake	-112.492	64.6574	17.7	429	3.2	16740	85.14
Creek Lake	-114.01	62.4733	0.88	-	-	774	79.55
Criss Lake	-113.514	63.0824	0.11	320	2.4	51	45.45
Croft Lake	-104.216	62.1037	15.74	337	6.4	14405	82.34
Crooked Foot Lake	-113.554	64.1502	9.02	374	8.2	8807	87.92
Cruikshank Lake	-105.357	63.5315	10.7	313	4.7	10138	85.23
Danes Lake	-111.706	63.2228	2.79	426	6.5	2398	77.42
DAoust Lake	-108.915	62.1353	11.25	333	10.9	11028	88
Daran Lake	-115.06	64.0299	20.75	257	37.7	19570	84.87
Darrell Lake	-105.65	63.7836	21.19	341	6.7	17950	76.26
Dauphinee Lake	-114.721	63.8824	9.95	288	13	9300	84.12
David lake	-114.378	62.5436	0.13	198	2.7	55	38.46
Davis Lake	-115.439	64.3984	1.33	335	10.8	1029	69.92
Day Lake	-113.504	62.6637	0.83	264	3.6	610	66.27
Defeat Lake	-113.643	62.3382	18.42	192	6.8	17144	83.77
Delmar Lake	-112.055	63.1382	8.65	406	8.1	7885	82.08
Denis Lake	-112.595	63.3542	7.34	387	9.2	6569	80.52
Desperation Lake	-112.401	62.5781	26.04	244	21.9	25205	87.1
Dessert Lake	-115.76	62.0993	7.68	202	4	7831	91.8
Devore Lake	-112.902	62.5951	0.94	270	4.5	738	70.21
Devreker Lake	-117.318	64.6627	13.12	235	24.8	12774	87.5
Dissension Lake	-113.499	63.983	4.97	336	5.3	4354	78.87
Dodds Lake	-113.424	63.1327	4.68	309	3.9	4020	77.35
Dome Lake	-113.255	62.7624	2.7	250	4.4	2166	72.22
Doodad Lake	-112.755	62.3539	0.27	257	2.1	133	44.44
Dorothy Lake	-112.534	62.4523	3.45	275	3	2744	71.59
Doyle Lake	-109.108	63.0974	13.79	352	13.4	12146	79.26
Drumlin Lake	-114.32	64.8287	36.46	437	5.4	34338	84.75
Drybones Lake	-112.405	63.5129	33.07	411	10.5	32593	88.69
Drygeese Lake	-114.166	62.734	3.74	217	7	3313	79.68
Drymeat Lake	-112.891	64.2536	7.92	379	6.7	7381	83.84
Duck Lake	-114.239	62.4336	5.38	155	6.6	4604	76.95
Duckfish Lake	-114.44	62.6736	5.79	228	5.3	4973	77.37
Dumas Lake	-116.301	66.4878	22.91	351	9.5	21601	84.85
Dumbell Lake	-111.083	64.0315	4.15	433	5.2	3571	77.35
Duncan Lake	-113.96	62.8705	68.2	214	21.4	70900	93.56
Egg Lake	-114.029	62.4897	0.91	192	3.7	638	62.64
Eileen Lake	-107.639	62.2437	135.71	369	9.6	128076	84.94
Elk River	-105.359	62.2166	59.41	337	4.4	49250	74.62

Ellington Lake	-117.32	65.0299	26.54	248	16.7	25216	85.49
Ernie Lake	-102.352	63.2671	20.99	252	12.2	21080	90.38
Etna Lake	-119.484	64.4488	45.73	356	3.3	46177	90.88
Eyeberry Lake	-104.696	63.1425	81.6	201	5.1	82207	90.67
Eyston Lake	-116.417	65.1823	23.89	298	27	22348	84.18
Faber Lake	-117.297	63.9325	383.34	203	22	402498	94.5
Face Lake	-110.126	62.3145	2.47	371	6.2	1750	63.56
Fairbairn Lake	-111.006	62.2618	14.6	169	12.8	14698	90.62
Fat Lake	-111.64	63.3964	12.85	412	7.5	11492	80.47
Faulkner Lake	-112.275	62.1985	2.37	204	9.6	1906	72.57
Fawn Lake	-117.529	62.1864	24.82	179	3.3	25619	92.91
Fenton Lake	-112.953	63.0183	16.2	277	23.1	15743	87.47
Fenwick Lake	-119.1	65.3622	3.14	205	11.1	2890	82.8
Fiddlers Lake	-114.509	62.468	0.28	192	2.2	196	64.29
Finger Lake	-114.357	62.5751	0.05	-	-	10	20
Fishhook Lake	-115.236	64.0626	8.4	262	19.2	7584	81.31
Fletcher Lake	-108.763	63.5923	164.24	388	11.6	164217	89.99
Forcier Lake	-116.351	66.0568	10.1	371	9.5	9373	83.56
Ford Lake	-107.409	63.1433	35.02	389	4	33188	85.29
Fortune Lake	-115.183	64.4511	0.36	353	4.4	232	58.33
Fox Lake	-114.417	62.483	0.52	199	2.7	359	61.54
Frame Lake	-114.391	62.4542	0.85	186	3.4	523	55.29
Francois Lake	-112.373	62.461	24.16	269	6.1	24259	90.36
Frodsham Lake	-113.604	63.6462	23.34	336	11.8	23316	89.8
Gagnon Lake	-110.45	62.0308	22.99	317	19.8	19590	76.69
Gale Lake	-115.268	63.9338	1.1	277	7.6	863	70.91
Gamey Lake	-115.204	64.1352	0.54	328	5.5	370	61.11
Gar Lake	-114.373	62.5212	0.28	182	2.9	188	60.71
Garde Lake	-106.268	62.832	104.05	-	-	99319	85.91
Gardenia Lake	-105.893	62.0199	40.35	361	5	36955	82.43
Georic Lake	-112.984	63.1825	0.6	324	6.2	398	60
Germaine Lake	-114.609	63.2969	22.84	265	16.2	20542	80.95
Ghost Lake	-115.147	63.8504	62.93	275	34.9	59083	84.49
Giauque Lake	-113.831	63.1809	16.46	252	22.8	15472	84.57
Glowworm Lake	-109.24	64.6365	102.5	412	20.4	102052	89.61
Gold Lake	-107.949	64.7369	2.87	325	14.4	2113	66.2
Goodspeed Lake	-109.465	63.098	57.92	319	24.2	53085	82.49
Goodwin Lake	-114.088	63.0453	2.82	248	7.4	2484	79.43
Gordon Lake	-113.201	63.0668	167.16	284	11.5	157999	85.07
Grace 2 Lake	-112.564	62.1628	3.7	218	5.7	3093	75.14
Grace Lake	-114.448	62.4188	0.64	172	3.4	378	53.12
Graham Lake	-113.807	62.9008	16.37	216	17.8	16453	90.47
Gras Lake	-110.448	64.523	705.63	404	9.6	724732	92.44
Great Slave Lake	-113.243	62.2183	9553.89	148	59.1	8607738	53.14
Greenrock Lake	-116.512	65.9309	2.8	394	7.8	2399	77.14
Greyling Lake	-114.289	62.6827	0.5	198	5.9	274	50
Grizzle Bear Lake	-112.982	64.1998	21.13	376	5.6	20776	88.36
Grizzly Lake	-115.574	64.5081	4.6	327	11.9	4108	80.43
Grodsky Lake	-108.391	62.082	5.87	372	3.7	5652	86.54
Hair Lake	-110.048	62.4313	5.24	185	16.8	4952	85.11
Hanbury Lake	-105.698	63.5646	7.57	328	8	7295	86.79
Handle lake	-114.397	62.4914	0.21	196	2.3	116	47.62
Handley Page Lake	-116.777	65.9876	29.03	315	17.3	28307	87.77
Hansen Lake	-116.748	65.6957	16.33	323	17.6	15363	84.69
Harald Lake	-113.535	62.685	4.12	260	3.3	3060	66.75
Hardisty Lake	-117.676	64.5506	302.59	186	26.9	298804	88.86
Harrison Lake	-107.659	63.0102	4.71	402	3.9	3464	66.24
Havant Lake	-115.555	65.8333	9.79	401	7.8	9524	87.33
Haywood Lake	-110.504	63.4599	32.79	395	8.2	32691	89.72
Healey Lake	-106.663	64.2964	153.4	352	8.2	141117	82.67
Heuss Lake	-107.081	63.3052	9.63	360	6.1	7831	73.21
Hidden 1 Lake	-113.682	62.5107	0.2	193	5	104	45
Hidden Lake	-113.556	62.5531	12.45	205	14.7	12189	88.11
Hilltop Lake	-111.041	63.3671	25.91	407	5.7	23714	82.36

Hislop Lake	-116.927	63.5189	34.04	172	14.6	33779	89.28
Hoare Lake	-105.131	63.6208	8.66	305	5	7769	80.72
Holmason Lake	-115.024	63.9889	1.27	269	13.9	1065	75.59
Homer Lake	-114.286	62.6641	0.59	-	-	358	54.24
Hottah Lake	-118.484	65.0678	842.81	175	6.7	875662	93.45
Howard Lake	-105.97	62.213	186.86	345	4	172970	83.31
Huff Lake	-107.163	62.2876	7.96	387	4.9	6599	74.62
Hump Lake	-116.552	63.586	2.72	191	8.2	2111	69.85
Humpy Lake	-113.435	64.6678	23.77	402	8.2	23502	88.98
Hunter Lake	-113.371	64.1024	9.9	362	8.9	9181	83.43
Indian Hill Lake	-110.736	63.222	90.09	380	4.1	82097	82.02
Indian Mountain Lake	-111.004	63.1267	23.55	387	15.6	21855	83.52
Indin Lake	-115.151	64.2435	156.43	253	45.2	150631	86.66
Inglis Lake	-115.164	63.1693	16.49	201	17.2	13740	75.02
Ingray Lake	-116.171	64.2701	139.71	241	62.9	142207	91.6
Irritation Lake	-115.264	65.0587	4.3	382	7.1	4019	84.19
Isabella Lake	-117.697	64.8136	59.6	186	26.9	60442	91.19
Island Lake	-114.1	62.4914	0.9	205	3.3	563	56.67
Itchen Lake	-112.827	65.5184	137.71	400	23.1	144870	94.68
Jackfish Lake	-114.392	62.4666	0.47	182	5	376	72.34
Jackson Lake	-114.305	62.5872	0.92	182	5.2	654	64.13
James Lake	-116.439	63.0095	19.34	147	15.8	17730	82.52
Jennejohn Lake	-113.747	62.4206	16.98	196	4.6	15192	80.51
Jim Lake	-104.579	62.4087	20.33	282	5.7	20581	91.1
Joe Lake	-114.387	62.483	0.1	-	-	45	40
Johnston Lake	-114.2	62.9965	5.34	213	10.6	4969	83.71
Jolly Lake	-111.94	64.1417	73.43	403	9.8	75697	92.78
Jones Lake	-108.377	62.3131	4.53	367	7.7	3984	79.25
Kam Lake	-114.406	62.4205	2.12	163	4.7	1770	75
Kamilukuak Lake	-102.005	62.4711	0.34	247	21.1	235	61.76
Keskarrah Lake	-115.25	66.0464	18.73	399	8.3	17792	85.37
King Lake	-110.762	63.7752	13.04	402	5.7	12294	84.82
Kirk Lake	-109.066	63.7188	64.1	389	5.7	64275	90.25
Kog lake	-114.396	62.4048	0.63	170	3.3	349	49.21
Koropchuk Lake	-116.767	64.1512	27.7	241	9.4	23818	77.4
Kway Cha Lake	-118.552	65.4413	23.96	166	2.8	23902	89.69
La Loche Lakes	-110.877	62.006	2.65	301	6.3	2423	82.26
Lac Avril	-115.292	63.9542	1.35	253	9.9	1123	74.81
Lac de Charloit	-107.976	63.8105	102.31	375	13.5	104407	91.85
Lac du Bois	-105.76	63.6146	13.71	343	3.8	12312	80.82
Lac Grandin	-119.064	63.9802	244.36	319	6.1	263747	97.14
Lac la Martre	-117.961	63.3195	1676.65	249	10	1815957	97.34
Lac la Prise	-108.722	63.062	30.61	375	9.9	29779	87.55
Lac Levis	-117.951	62.6347	53.25	265	3.7	56088	94.8
Lac Malfait	-117.988	64.6284	38.05	174	4.8	38337	90.67
Lac Nez Croche	-111.403	63.2502	28.59	396	9.7	27563	86.78
Lac Tachs	-119.987	64.0127	124.55	308	13.5	126349	91.3
Lac Tate dOurs	-110.572	63.3577	62.23	385	10	63718	92.16
Lake of the Enemy	-110.238	63.7792	135.33	396	12.2	134187	89.06
Lake Providence	-112.065	64.7582	102.58	358	28	103207	90.55
Lamoureux Lake	-113.682	62.9108	4.11	270	6.1	3551	77.86
Landing Lake	-114.408	62.56	1.28	202	2.6	861	60.16
Languish Lake	-112.904	62.7684	11.24	307	4.4	10597	84.88
Larocque Lake	-107.707	63.0496	1.5	396	2.5	1108	66.67
Lastfire Lake	-113.029	64.5342	6.13	357	6.4	5919	86.95
Laurie Lake	-115.208	64.4817	0.47	358	5	330	63.83
Lausen Lake	-109.744	62.5875	7.24	186	15.3	6648	82.6
Leonforte Lake	-119.654	64.5848	10.65	392	6.1	10916	92.21
Likely Lake	-114.311	62.6466	0.39	204	4.9	130	30.77
Little Crapeau Lake	-116.518	64.8211	123.5	275	21.4	118280	85.98
Little Forehead Lake	-113.281	64.7824	18.2	401	20	16804	83.08
Little Lake	-113.96	62.5467	0.14	217	2.7	92	57.14
Logie Lake	-105.759	62.1353	4.23	357	2.8	3454	73.52
Long Lake	-114.442	62.4773	1.16	196	2.1	788	61.21

Long Legs Lake	-113.773	64.7613	16.7	417	5.6	14850	80.06
Longtom Lake	-117.834	65.1715	43.93	189	19.3	43869	89.87
Lou Lake	-116.782	63.5682	1.82	193	13.8	1468	72.53
Love Lake	-114.759	62.995	4.43	246	5.9	3172	64.33
Lynx Lake	-106.285	62.4099	295.27	344	10.1	282676	86.16
Mac Lake	-113.468	63.0753	5.09	312	5.3	3993	70.53
MacKay Lake	-111.012	63.9233	972.33	390	20.7	1002573	92.8
MacLellan Lake	-110.037	63.2324	23.2	383	13.9	20923	81.16
MacNaughton Lake	-115.314	63.7135	0.37	296	3.7	201	48.65
Mad Lake	-112.749	62.1169	1.16	222	4.1	958	74.14
Madeline Lake	-114.081	62.5468	0.93	170	8.8	733	70.97
Magpie Lake	-108.877	62.4488	4.13	355	8.8	3700	80.63
Magrum Lake	-108.635	62.0674	4.97	373	7.1	4492	81.29
Malley Lake	-108.087	63.5601	30.34	395	7.5	25931	76.93
Mann Lake	-112.797	62.3496	1.26	244	2.2	958	68.25
Mantic Lake	-104.457	62.3336	59.48	293	5.4	58030	87.81
Margaret Lake	-117.128	64.507	102.43	203	32.2	101844	89.47
Marian Lake	-116.203	62.9243	236.84	147	15.8	251024	95.22
Martin Lake	-114.439	62.5313	3.09	197	3.2	2163	63.11
Mary Frances Lake	-106.245	63.3043	149.45	363	8	143654	86.51
Mary Lake	-103.54	62.3855	164.8	294	20.6	170394	92.96
Mattberry Lake	-115.891	64.1132	82.24	235	38.6	80356	87.94
Matthews Lake	-111.245	64.0696	10.35	422	6.3	9582	83.29
Max Ward Lake	-113.708	65.4787	11.65	367	8.5	11912	92.02
Maze Lake	-105.944	63.8946	16.16	350	2.9	12516	69.68
Mazenod Lake	-117.014	63.7003	36.3	199	14	34834	86.36
McCrea Lake	-112.572	63.5556	16.07	404	12	15065	84.38
McIntosh Lake	-114.901	65.7574	3.71	436	5	3398	82.48
McKee Lake	-110.043	62.3492	2.97	353	6.1	2387	72.39
McKinlay Lake	-111.541	62.8749	26.65	365	8.1	25518	86.19
McKinnon Lake	-108.497	62.0601	10.03	370	5.6	9324	83.65
McLellan Lake	-117.958	63.8428	9.55	-	-	9510	89.63
McPhee Lake	-113.052	63.0264	1.91	312	7.2	1323	62.3
McTavish Arm	-117.83	65.4491	189.7	175	29.6	188745	89.55
Meander Lake	-112.149	62.5774	10.48	311	10.7	9539	81.97
Meg Lake	-114.383	62.416	0.09	-	-	45	44.44
Meridian Lake	-109.43	62.6042	37.1	201	26.3	38923	94.42
Merl Lake	-112.655	62.4007	0.7	260	3.5	550	70
Mesa Lake	-115.147	64.8268	36.55	365	12.4	34701	85.44
Messina Lake	-119.526	64.1837	18.27	371	7	18633	91.79
Methane Lake	-114.174	62.4838	0.98	180	3.8	684	63.27
Michel Lake	-114.141	62.881	3.17	229	6.1	2633	74.76
Milner lake	-114.341	62.5923	0.41	212	2.3	182	39.02
Misty Lake	-109.785	63.067	9.86	321	12.9	9180	83.77
Moberly Lake	-114.315	63.0166	12.75	225	20.8	10564	74.59
Mohawk Lake	-112.115	64.0222	20.01	438	4.6	18774	84.46
Moise Lake	-114.136	62.3247	0.78	166	3.7	596	69.23
Moose Lake	-114.089	62.9803	1.24	253	5.7	978	70.97
Moraine Lake	-106.01	64.1074	80.99	352	5.3	75416	83.8
Morel Lake	-113.677	65.6372	20.28	380	8	19808	87.92
Morose Lake	-112.915	62.8252	12.01	311	6	11015	82.51
Mosquito Lake	-103.341	62.5798	311.21	292	12.7	323804	93.54
Mud Lake	-117.197	63.0225	11.2	-	-	9829	79.02
Munn Lake	-109.974	63.6481	70.94	391	15.9	71057	90.01
Murdock Lake	-109.431	63.5811	51.1	423	4	44286	78
Murphy Lake	-109.801	62.1121	8.86	299	9.4	8198	83.3
Murray Lake	-113.441	63.0154	2.56	292	3.7	2187	76.95
Musclow Lake	-106.953	63.7879	4.97	375	3.2	4259	77.06
Muskeg Lake	-103.64	62.0805	8.47	322	5.4	6939	73.67
Naga Lake	-119.21	65.2199	5.31	175	5.7	5261	89.08
Nardin Lake	-113.839	63.4931	18.14	341	11.9	15645	77.62
Nelligan Lake	-105.784	63.3149	8.66	360	4.1	7482	77.71
Nelson Lake	-108.111	62.1925	7.77	409	3.5	5840	67.7
Newbigging Lake	-112.226	64.4419	15.36	444	8	15039	88.15

Nieznany Lake	-105.175	62.3904	3.56	323	3.9	2966	75
Nonacho Lake	-109.317	62.0843	104.88	312	15.3	104841	89.86
NoName Lake 01	-114.39	62.5522	0.06	-	-	14	16.67
NoName Lake 02	-108.095	64.4885	50.13	379	14.1	48651	87.35
NoName Lake 03	-109.052	64.3012	28.16	403	4.6	28308	90.48
NoName Lake 04	-109.297	64.3279	64.28	393	6.3	65424	91.6
NoName Lake 05	-108.275	63.7958	20.95	389	6.2	20814	89.4
NoName Lake 06	-112.075	63.6362	70.68	413	7.3	68296	86.97
NoName Lake 07	-110.554	63.5828	64.99	409	8.4	59077	81.81
NoName Lake 08	-114.046	63.3532	17.4	290	28.3	16528	85.52
NoName Lake 09	-107.279	63.3114	77.05	362	6.1	74521	87.05
NoName Lake 10	-106.178	63.1366	47.57	349	5.9	47674	90.2
NoName Lake 11	-117.93	62.9845	45.5	267	3.1	46436	91.85
NoName Lake 12	-102.796	63.0017	88.98	263	4.3	86218	87.21
NoName Lake 13	-111.917	62.9299	40.08	390	13.8	39749	89.25
NoName Lake 14	-102.003	62.6587	34.76	246	8.7	31634	81.9
NoName Lake 15	-114.246	62.7732	24.89	195	21.1	20640	74.65
NoName Lake 16	-113.936	62.5755	38.89	166	20.8	36375	84.19
NoName Lake 17	-114.194	62.5985	36.73	152	24.4	36116	88.48
NoName Lake 18	-107.594	62.4351	48.91	362	8.7	46675	85.89
NoName Lake 19	-103.28	62.2774	62.81	285	8.5	60275	86.29
NoName Lake 20	-114.47	62.6374	1.1	215	4	661	53.64
NoName Lake 21	-114.421	62.5109	1.33	201	1.6	919	62.41
NoName Lake 22	-114.231	62.4853	3.21	169	5.3	2700	75.7
NoName Lake 23	-114.177	62.4598	1.39	164	2.9	1069	69.06
NoName Lake 24	-114.628	62.428	1.26	171	2.6	891	63.49
NoName Lake 25	-114.472	62.5003	0.21	204	1.9	131	57.14
NoName Lake 26	-109.632	65.0632	208.76	427	15.1	208919	89.95
NoName Lake 27	-110.876	64.792	109.48	430	8.2	108844	89.48
NoName Lake 28	-115.883	63.7155	139.74	208	2	129795	83.48
NoName Lake 29	-112.318	63.4001	106.08	397	14.5	100296	85.1
NoName Lake 30	-102.65	62.5706	194.39	255	11.7	192351	89.06
NoName Lake 31	-114.871	65.2597	25.88	449	5.6	25720	89.45
NoName Lake 32	-115.923	65.0306	54.52	348	18.5	52898	87.33
NoName Lake 33	-109.082	65.024	68.24	399	10.9	71432	94.21
NoName Lake 34	-108.844	64.9761	36.5	380	7.7	38642	95.29
NoName Lake 35	-109.044	64.9043	19.27	417	12.8	19406	90.66
NoName Lake 36	-108.66	64.9469	44.71	382	6.7	45389	91.37
NoName Lake 37	-109	64.7693	65.26	397	9.9	64212	88.55
Noyes Lake	-105.901	62.5395	24.79	346	4.3	24435	88.71
Octopus Lake	-114.449	62.3737	0.77	158	1.8	453	53.25
Odjick Lake	-113.917	65.516	31.55	358	28	32155	91.73
Old Canoe Lake	-111.453	63.443	61.76	421	12.5	57663	84.03
Olson Lake	-105.277	62.9121	7.97	337	4	7755	87.58
One Arm Lake	-114.342	62.5458	0.12	183	3	37	25
Orkney Lake	-113.182	64.1307	5.96	385	5	5583	84.23
Oro Lake	-114.333	62.6283	0.46	219	3.5	231	45.65
Ortona Lake	-119.222	64.7705	14.3	634	6.2	14279	89.86
Outram Lakes	-109.433	64.0362	48.87	367	9.2	49430	91.04
Papanakies Lake	-110.338	63.2306	23.3	406	5.7	22211	85.79
Parent Lake	-114.381	65.2658	50.14	376	14.6	49992	89.73
Pate Lake	-114.206	64.4237	12.02	382	7.4	11154	83.53
Payne Lake	-112.068	62.8293	9.74	362	12.1	8904	82.24
Peaceful Lake	-113.505	62.9932	2.46	283	4.2	2119	77.64
Pellatt Lake	-109.777	64.9606	40.31	427	15.1	38887	86.83
Pelonquin Lake	-111.225	65.3221	21.08	493	7	21342	91.13
Peninsula Lake	-113.364	62.5234	0.84	230	4.2	501	53.57
Perlson Lake	-111.92	63.1328	24.87	394	9.1	24483	88.58
Phoenix Lake	-113.339	63.7636	27.15	344	13.9	24178	80.15
Pickerel Lake	-113.488	62.4943	1.57	209	6.8	1100	63.06
Pink Lake	-113.018	62.6731	3.44	263	7.4	2883	75.29
Plant Lake	-113.557	62.5236	5.31	212	7.9	5901	84.16
Plex Lake	-110.785	63.1137	2.21	389	5.8	2036	82.81
Point Lake	-113.091	65.2602	626.84	358	28	644500	92.47

Pollock Lake	-115.808	63.3195	4.06	198	9.3	3165	70.2
Pontoon Lake	-114.003	62.5418	3.36	195	7.2	3064	82.14
Porphyry Lake	-113.403	64.0488	3.53	345	6.9	3156	80.45
Prang Lake	-112.501	63.8773	14.34	425	7.9	13060	81.94
Preg Lake	-114.081	62.4527	0.17	173	3.3	76	41.18
Prestige Lake	-113.645	62.9615	8.25	270	6.8	7802	85.09
Price Lake	-108.158	62.0349	8.59	375	7	8341	87.43
Ptarmigan Lake	-107.429	63.5903	82.73	352	12.7	82480	89.71
Pud lake	-114.383	62.4316	0.17	181	2.7	96	52.94
Rabbit Lake	-116.849	63.4668	11.96	172	12.4	12441	93.65
Raccoon Lake	-117.692	62.87	43.93	287	1	45951	94.15
Radford Lake	-105.576	63.3944	41.05	341	4.5	39226	85.99
Rae Lake	-117.321	64.1656	201.35	200	28.3	198474	88.72
Range Lake	-114.423	62.4473	0.21	188	2.9	110	47.62
Ranji Lake	-115.09	64.1015	15.29	260	29.8	15364	90.45
Rater Lake	-114.368	62.5537	0.2	182	3.8	51	25
Rawalpindi Lake	-114.623	65.0285	88.37	415	6.7	87345	88.96
Rebesca Lake	-116.373	64.5352	65.24	252	36.5	66388	91.46
Recluse Lake	-114.015	66.0421	0.71	376	13.5	522	66.2
Redout Lake	-113.016	62.7403	8.38	293	7.4	7423	79.71
Redrock Lake	-114.165	65.4776	83.25	358	28	82622	89.32
Reid Lake	-109.959	63.7626	40.8	401	8.9	39960	88.14
Reindeer Lake	-113.583	63.8865	50.25	338	10.5	49658	88.94
Rib Lake	-114.177	62.3445	0.58	166	4	430	67.24
River Lake	-114.091	62.5945	4.96	166	20.8	4495	81.65
Robb Lake	-116.021	65.3709	16.95	356	15.4	17118	90.91
Robert Lake	-109.357	62.3803	3.52	331	11.8	2948	75.28
Rodrigues Lake	-115.633	64.7871	5.55	296	11.5	5399	87.57
Rolfe Lake	-111.725	63.0835	55.57	402	8.2	54011	87.48
Rome Lake	-118.342	64.3155	22.23	402	3.3	21396	86.64
Ross Lake	-113.26	62.6815	15.7	254	7	14207	81.46
Roulante Lake	-113.748	64.5571	20.52	420	11.4	18449	80.9
Roundrock Lake	-113.404	64.3891	29.74	342	23.9	29970	90.69
Rupp Lake	-112.264	63.8287	6.37	442	4.8	5234	73.94
Russell Lake	-115.75	63.0373	177.03	147	15.8	171240	86.93
Ryan Lake	-114.372	62.5871	1.06	220	2.6	879	74.53
Samandr Lake	-115.384	65.9782	59.36	422	10.8	59573	90.11
Sandy Lake	-113.077	64.1536	4.18	382	6.6	3763	80.86
Sarah Lake	-117.147	63.7832	66.45	187	17.3	66049	89.45
Savannah Lake	-108.911	64.4309	29.02	393	6.6	27969	86.73
Savoy Lake	-115.436	64.4286	1	330	7.7	773	70
Schist Lakes	-109.913	62.3707	0.95	353	5.2	422	40
Scott Lake	-113.572	62.652	2.62	246	5.6	1883	64.5
Scotty Lake	-112.989	63.4673	1.67	408	8.6	1359	73.05
Seahorse Lake	-111.229	64.3086	20.41	420	5.4	20629	90.98
Seal Lake	-108.95	64.6326	83.6	403	13.1	79887	86
Second Lake	-117.426	62.1259	3.27	179	5.4	3122	85.93
Self Lake	-117.274	65.2949	21.46	292	14.3	20770	87.09
Shadow Lake	-114.35	62.5662	0.06	-	-	13	16.67
Shamrock Lake	-115.012	64.7763	17.82	367	8.9	17503	88.38
Shaw Lake	-112.765	64.6106	4.99	392	6.2	4290	77.35
Short Point Lake	-114.224	62.7569	5.69	195	21.1	5339	84.53
Sid Lake	-103.986	62.2425	289.48	296	12	304865	94.78
Sifton Lake	-106.36	63.7027	90.93	355	6.6	75978	75.2
Simon Lake	-117.318	65.5421	6.98	270	11.8	6211	80.09
Singing Lake	-112.925	64.3162	13.32	370	9	12863	86.79
Sled Lake	-106.821	62.1265	23.5	380	6.4	21841	83.66
Sleepy Dragon Lake	-112.909	62.9194	5.21	331	5.7	4748	81.96
Slemon Lake	-116.033	63.2081	44.91	138	14.7	44378	88.82
Small Lake	-113.826	62.5185	0.74	193	5.1	547	66.22
Smart Lake	-106.822	63.4912	112.35	356	11.3	103542	82.88
Smoky Lake	-116.495	65.9003	2.45	369	9.8	2178	80
Snelgrove Lake	-105.615	62.3356	7.59	348	4.4	6599	78.26
Sophia Lake	-114.121	62.9357	3.64	248	7.2	2327	57.42

Sosan Lake	-111.95	63.2369	5.26	432	4.6	4140	70.91
Sparrow Lake	-113.648	62.6144	12.58	237	6.4	12077	86.41
Spencer Lake	-112.462	63.1573	13.2	375	11.8	13060	88.86
Sphinx Lake	-115.366	64.4645	1.56	345	5.7	1351	78.21
Spider Lake	-115.145	64.5067	16.58	341	11.5	13690	74.31
Sproule Lake	-113.478	62.7444	1.6	274	2.4	1022	57.5
Spruce Island Lake	-110.427	62.4009	1.66	171	10.3	1419	77.11
Staple Lake	-114.033	62.729	1.27	247	3.1	822	58.27
Starfish Lake	-111.61	64.3321	21.29	403	6.3	21575	91.22
Starvation Lake	-112.731	64.8988	37.76	400	9.1	38344	91.39
Steel Lake	-104.593	63.7203	8.98	159	8.6	8562	85.86
Sterlet Lake	-109.496	64.7214	44.66	426	15.1	41175	82.89
Street Lake	-105.317	63.4127	15.43	326	2.8	13352	77.9
Sunken Lake	-110.233	62.9846	1.7	259	19.1	1460	77.06
Suse Lake	-112.966	63.1386	2.36	341	4.8	1975	75.42
Sussex Lake	-108.328	64.4388	14.31	379	22	13522	85.05
Tanco Lake	-112.223	62.4201	4.27	272	5.7	2945	62.06
Tarantula Lake	-107.95	64.521	39.79	373	7.7	38615	87.33
Taylor Lake	-108.664	63.7853	33.13	389	10.2	32402	88.02
Tayonton Lake	-116.544	63.2112	23.03	150	3.6	12081	47.2
Tent Lake	-107.957	62.4281	72.1	346	12.7	67843	84.69
Terry Lake	-113.31	62.511	4.28	226	3.5	2570	53.97
The Nine Lakes	-114.043	63.4579	1.59	324	5.8	1194	67.3
Thetis Lake	-113.275	63.7214	29.11	351	9.9	28312	87.36
Thistlethwaite Lake	-113.627	63.1591	44.27	252	22.8	42541	86.49
Thomas Lake	-119.187	65.1207	3.81	241	3.8	3568	83.99
Thompson Lake	-113.5	62.6137	2.81	252	2.9	2381	76.16
Thonokied Lake	-109.628	64.3849	129.5	394	18.3	127553	88.55
Timberhill Lake	-106.655	62.37	16.55	363	6.3	14940	81.27
Toad Lake	-111.746	62.7272	5.91	362	4.8	4883	74.28
Tonggot Lake	-119.697	63.9928	18.55	312	4.3	15529	75.36
Toopon Lake	-110.439	62.3529	1.51	176	9.1	1372	81.46
Torrie Lake	-116.926	66.2355	0.52	310	7.7	430	75
Toura Lake	-108.568	62.8338	0.79	374	5	507	58.23
Trapper lake	-114.363	62.5266	0.31	182	3.1	137	38.71
Trout Lake	-114.364	62.7997	2.82	204	10.3	2400	76.6
Truce Lake	-114.886	64.5323	28.65	343	8.4	27814	87.36
Trumper Lake	-117.582	63.5949	4.96	-	-	4201	76.21
Tsan Lake	-112.937	64.0169	12.79	374	5.6	11773	82.88
Tuchay Lake	-119.163	65.2513	31.72	172	11.1	31222	88.56
Tuche Lake	-117.317	64.3356	14.78	200	15.8	14489	88.23
Tumi Lake	-116.794	63.4535	6.07	165	7.7	5620	83.36
Tyrrell Lake	-105.498	63.1246	227.09	318	9.8	220532	87.4
Uhlman Lake	-116.799	66.1321	9.3	314	12	8538	82.58
Upper Pensive Lake	-113.393	62.7247	3.28	246	5	2718	74.7
Upper Ross Lake	-113.153	62.7296	9.22	254	7	8451	82.54
Ursula Lake	-110.459	64.8159	22.95	453	6.7	22803	89.41
Vaillant Lake	-114.51	66.2053	2.46	329	11.2	2230	81.71
Van Lake	-113.077	63.3649	4.48	340	11.5	3780	75.89
Vee Lake	-114.35	62.5555	0.7	178	4.4	393	50
Victory Lake	-113.077	62.6708	10.37	252	4.2	9373	81.39
Vital Lake	-114.438	62.601	1.49	194	5.3	1092	65.77
Waite Lake	-113.322	62.8342	7.62	290	3.7	5495	64.96
Wallie Lake	-113.951	63.1343	0.2	285	3.4	98	45
Walmsley Lake	-108.493	63.4197	231.36	378	25.8	233258	90.74
Walsh Lake	-114.281	62.5829	9.17	174	9.6	8030	78.84
Webb Lake	-113.125	62.8492	3.62	314	4.6	2650	65.75
Wecho Lake	-113.812	63.9602	102.43	351	16.2	97862	85.99
Wedge Lake	-113.69	62.8632	9.87	260	7.9	8665	79.03
White Quartz Lake	-108.383	62.6897	2.6	380	6.1	2089	72.31
Whitefish Lake	-106.802	62.6983	331.46	350	11.6	326891	88.68
Whitewolf Lake	-113.919	64.9647	52.93	419	10.1	47837	81.33
Willow Lake	-114.215	62.3617	0.9	162	5.5	658	65.56
Windflower Lake	-118.517	62.8653	36.65	256	3.7	38202	93.81

Windy Lake	-109.928	64.9443	8.61	440	7.4	8000	83.62
Winter Lake	-112.943	64.4877	45.27	346	11.6	46846	93.09
Wolverine Lake	-111.38	63.2084	23.42	396	9.7	23074	88.68
Wonnacott Lake	-116.686	63.7158	1.62	-	-	1028	57.41
Woyna Lake	-112.985	62.4704	2.52	241	6	2226	79.37
Wylie Lake	-117.011	65.6689	15.66	322	9.4	14391	82.69
Yamba Lake	-111.376	64.9531	305.28	403	16.7	310925	91.66
Yanik Lake	-118.631	65.3664	8.1	230	5.2	8157	90.37
Zebulon Lake	-117.853	65.0521	56.04	184	15.4	56562	90.85
Zigzag Lake	-113.035	62.3407	5.11	200	10.9	4239	74.76
Zinto Lake	-116.396	64.1152	52.42	242	27.9	48637	83.5
Zipper Lake	-112.522	63.7092	3.81	426	6.5	3055	72.18
Zucker Lake	-106.799	62.9326	53.17	373	4.2	47658	80.67

625